TWO OUTPUT SERIES RESONANT INVERTER FOR INDUCTION HEATING AND INDUCTION COOKING APPLICATION

A THESIS SUBMITTED TO THE GRADUATE SCHOOL OF APPLIED SCIENCES OF NEAR EAST UNIVERSITY

By

SALIH MOUSAY ALI ABRAHEEM

In Partial Fulfilment of the Requirements for the Degree of Master of Science in Electrical and Electronic Engineering

NICOSIA

2020

TWO OUTPUT SERIES RESONANT INVERTER OF INDUCTION HEATING AND INDUCTION COOKING APPLICATION

A THESIS SUBMITTED TO THE GRADUATE SCHOOL OF APPLIED SCIENCES OF NEAR EAST UNIVERSITY

By

SALIH MOUSAY ALI ABRAHEEM

In Partial Fulfilment of the Requirements for the Degree of Master of Science in Electrical and Electronic Engineering

NICOSIA

2020

SALIH MOUSAY ALI ABRAHEEM: TWO OUTPUT SERIES RESONANT INVERTER OF INDUCTION HEATING AND INDUCTION COOKING APPLICATION

Approval of Director of Graduate School of Applied Sciences

Prof. Dr. Nadire Cavus

We certify this thesis is satisfactory for the award of the degree of Master of Science in Electrical and Electronic Engineering

Examining Committee in Charge:

Prof. Dr. Senol Bektas	Committee Chairman, Department of Electrical and Electronic Engineering,NEU
Prof. Dr. Seyedhossein Hosseini	Supervisor, Department of Electrical and Computer Engineering, University of Tabriz-Iran
Assist. Prof. Dr. Sertan Serte	Department of Electrical Engineering,NEU

I hereby declare that all information in this document has been obtained and presented in accordance with academic rules and ethical conduct. I also declare that, as required by these rules and conduct, I have fully cited and referenced all material and results that are not original to this work.

Name, Last name: Salih Mousay Ali Abraheem

Signature:

Date:

ACKNOWLEDGEMENTS

I would like to express my special thanks of gratitude to my supervisor Prof. Dr Seyedhossein Hosseini, Near East University, Northern Cyprus, for giving me the opportunity to conduct this research by providing invaluable guidance throughout the process.

I would like to express my deepest thanks to the head of the Electrical and Electronic Engineering Department Prof. Dr. Bulent Bilgehan.

I pay my deep sense of gratitude to Prof. Dr.Senol Bektas to provide me the opportunity to defense my thesis this semester.

I grateful to my advisor Dr. Sertan Serte, and it is always a pleasure to remind the fine people in Near East University for their sincere guidance.

Last but not the least, I owe and respectfully offer my thanks to my father, mother, wife and my daughter for their constant moral support and mellifluous affection which helped me to achieve success in very sphere of life and without their kind devotion this thesis would have been a sheer dream.

ABSTRACT

Induction cooking systems have seen rapid developments over the past few years due to the numerous merits it possesses. Inverter are a critical component of the induction cooking systems; the appropriate and efficient application of these components will translate into higher efficient induction cooking systems and reduced cost of the systems. This research propose a single inverter with two outputs for multiple burner applications. The proposed topology is a high frequency series resonant based inverter. The proposed inverter eliminates the need for two H-Bridge structures to operate two loads. This topology is derived by adding two switches to the conventional H-Bridge structure and provides simultaneous or separate control of the two outputs hence minimum component quantity is achieved and therefore the proposed topology has minimum size and volume and reduced inverter cost. The series resonant tank provides minimum losses caused by switching hence the overall converter efficiency is increased. Analysis of the propounded topology investigated theoretically and simulation done in MATLAB R2015a environs.

***Keywords*:** Resonant tank, Induction heating, Two output inverter, multilevel inverter.

ÖZET

İndüksiyonlu pişirme sistemleri, sahip olduğu sayısız değer nedeniyle son birkaç yılda hızlı gelişmeler kaydetti. İnvertör, endüksiyonlu pişirme sistemlerinin kritik bir bileşenidir; bu bileşenlerin uygun ve verimli uygulanması daha yüksek verimli indüksiyonlu pişirme sistemlerine ve sistemlerin maliyetini düşürür. Bu araştırma, çoklu brülör uygulamaları için iki çıkışlı tek bir invertör önermektedir. Önerilen topoloji, yüksek frekanslı bir seri rezonans bazlı invertördür. Önerilen invertör, iki H-Köprüsü yapısının iki yük işletmesi ihtiyacını ortadan kaldırır. Bu topoloji, geleneksel H-Bridge yapısına iki anahtar eklenerek elde edilir ve iki çıkışın eşzamanlı veya ayrı kontrolünü sağlar, böylece minimum bileşen miktarı elde edilir ve bu nedenle önerilen topoloji minimum boyut ve hacme ve invertör maliyetine sahiptir. Seri rezonant tankı anahtarlamadan kaynaklanan asgari kayıpları sağlar, dolayısıyla genel dönüştürücü verimliliği artar. Elde edilen topolojinin analizi teorik olarak incelenmiştir ve simülasyonu MATLAB R2015a çevrelerinde yapılmıştır.

Anahtar Kelimeler: Rezonans tankı, İndüksiyonla ısıtma, İki çıkışlı invertör, çok seviyeli invertör.

TABLE OF CONTENTS

LIST OF FIGURE

.

LIST OF TABLES

LIST OF ABBREVIATIONS

AC : Alternating Current.

DC : Direct Current.

BJT : Bipolar Junctions Transistor.

EMI : Electromagnetic Interference.

PWM: Pulse Width Modulation.

MI : Multilevel inverter.

NPC : Neutral point clamped.

FC : Flying capacitor**.**

VSI : Voltage source inverter.

CSI : Current source inverter.

RC : Resonant converter.

ZVS : Zero voltage switching.

ZCS : Zero current switching**.**

CHAPTER 1

INTRODUCTION

1.1 Overview

Power electronic converters have become principal devices in providing of cheap, efficient, reliable and quality power to the consumer. Basically converters are useful devices in the chain of power supply, they are mostly suitable for power conditioning or providing power with the desired qualities as desired by the consumer of the load. Power electronic converter is the broad name used to describe the four devices (inverters, rectifiers, cycloconverter and choppers) mostly used in power conditioning. My research falls under the categories of inverters hence detailed description of this device will be described without mentioning the other three devices.

The conventional inverter is a 2-step inverter powered at the source by a voltage source. This topology of inverter functioned as a variable voltage or variable frequency device i.e. it uses constant dc voltage at the input to provide variable voltage and frequency at the output; this is achieved by utilizing appropriate switching methodology. Considering the type of input power, inverters are categorized into two groups; current source inverters (CSI) and voltage source inverters (VSI).

A VSI is obtained when the source or input side of the device is powered by a constant dc voltage. A VSI has a constant voltage but the output voltage is heavily dependent on the nature of characteristics of inverter; however the output current of the inverter is determined by the load type. VSI are the most common types of inverters because most applications require voltage source inverters, the principal application of inverters is change dc voltage in ac voltage, other applications of VSI are FACTS systems, variable speed drives, HVDC transmission systems, renewable energy system interfacing, traction, filtering. VSIs are most suitable for medium range power applications because of the quality of the output voltage produced. The dc voltage used as the input of the inverter can be derived from a rectifier circuit of any of the following sources; PV systems, capacitor, fuel cell, batteries etc. VSIs are commonly used in multilevel inverters (MI) because of the simple structure and control of most MI topologies. In cascaded topologies, multiple dc sources are required hence a combination of any of the above sources can be utilized. A common type of VSI circuit is the single phase H Bridge inverter with four switches each connected with an anti-parallel diode, this switch topology allows for current flow in bi-direction and unidirectional voltage flow.

Switching and conduction of power electronic switches produces undesirable factors which increases the cost, operation and maintenance of the converter. These undesirable factors are stresses during switching, losses occurring during switching and EMI interferences. To overcome these challenges, zero or zero current is desired during the period of switching. Several techniques such as application of snubber circuit have been proposed to achieve this goal, however the snubber circuit can be considered as dissipative hence not really efficient. The resonant converter topology is however more practical in achieving zero voltage/current during switching. The resonant converters are broadly categorized into four groups namely; load resonant converters, resonant switch converters, resonant dc-link converter and finally HF-half cycle converters. More emphasis will be laid on the LS converters; specifically on series resonant converters. The series resonant converter or inverter is a type of resonant tank which is composed of an inductor and capacitor connected in series between the main converter circuit and the load. Using the series load resonant converter will result in achieving zero current or voltage switching hence eliminate the problems associated with switching of power electronic converters.

Induction cookers are classified into the type of heating systems which functions under low power systems but having its output maximum power not exceeding 3kW for each connected load. However a new classification of induction cooker is proposed in (F. Z. Peng et al., 2002); the classification is based on power ratings greater or less than 1.2kW. Figure. 1a and Figure. 1b shows the two types of classification. The traditional induction cooking system is composed of a pan commonly called wok placed onto of coil; the coil is induction type and flat in nature. An insulator is used to separate the wok and the coil. The generated heat from the coil used in cooking is obtained from hysteresis losses and currents due to eddy phenomenon.

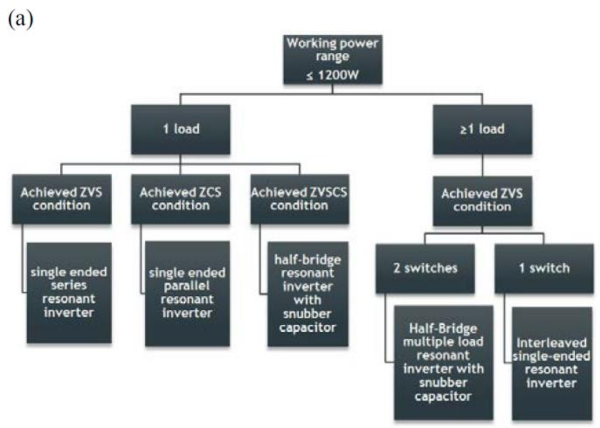

Figure. 1a: Induction cookers rated below 1.2kW (F.Z. Peng et al., 2002)

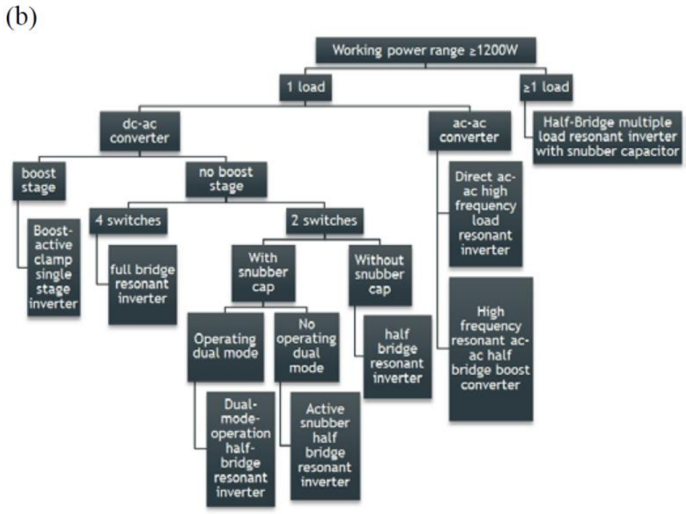

Figure. 1b: Induction cookers rated above 1.2kW (F.Z. Peng et al., 2002)

Induction cookers operate under medium power systems hence a frequency within this range with magnitude between 20 kHz to 100 kHz is used to generate current for powering the induction cooker. The transformer analogy is used in modeling the coupled woke and coil; and it’s described as a resistor and capacitor series connection. The desired maximum output power and the operating frequency is used to determine the magnitudes of the resistor and inductor. The input power or energy of the induction cooker is obtained from a dc voltage or a rectifier circuit, current of high frequency is supplied by the inverter circuit to the induction coil. Ripples are an integral component of the supplied current hence all components or devices utilized in this topology should have maximum ripple tolerance. Resonant converters for induction cooking can vary between different topologies such as the conventional H-Bridge circuit or its half topology, impedance based structures which provide more power to the load than any other type of inverter topology; this is basically due to the buck-boost functionality and the high gain provided by this topology.

The induction cooker can be a single burner cooker or multiple burner cooker where one, two, three or four burners are provided by one circuit of induction cooker. In the conventional multiple burner, one inverter is used to power one burner whiles the newer technologies uses one inverter for multiple burners, also another technique is to use one inverter with mechanical switch to power multiple burners. The desired circuit and its corresponding output waveform is shown by Figure. 2.

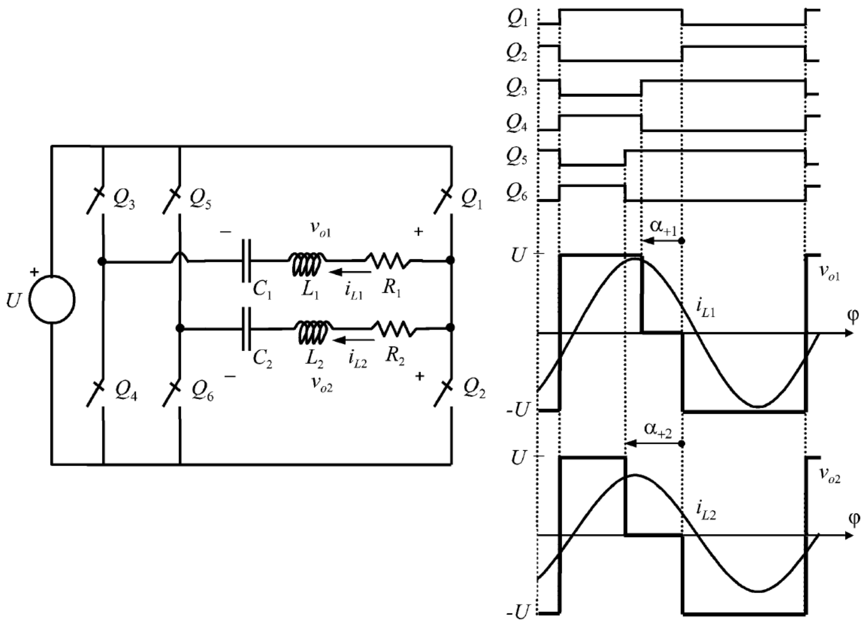

Figure. 2: Two output SLR converter with output waveforms (A. Nabae, H. Akgi et..1981)

1.2 Thesis Problem

The new trends in power electronic converters is to achieve the highest efficiency possible and this is derived by utilizing the minimum number of components which directly relates to reduce converter size, increased efficiency and reduced cost. Switching and conduction of power electronic switches produces undesirable factors which increases the cost of operation, reduces efficiency and maintenance of the converter. These undesirable factors are stresses during switching, losses occurring during switching and EMI interferences.

The resonant tank topology is included in converters to at achieve zero voltage or zero current during the period of switching; once this desired characteristics is achieved, the switching power is reduced to zero or the barest minimum hence switching losses are eliminated or minimized.

Snubber circuit can also be utilized to achieve this goal but the components of the snubber circuit are dissipative hence not efficient. Utilizing a converter with the least possible number of components the desire of current engineers.

1.3 The Aim of The Thesis

The aim of this thesis to simulate a two output series resonant inverter which is applicable in induction heating cooking; this topology can be applied in other applications. For this specific application as induction cooker, the desired characteristics or features are, SLR structure, two out inverter, variable voltage and frequency at the output. Utilizing PWM control method, each output of the two output will have independent control mechanism or the simultaneous control of the two outputs will be permissible. Also the desired maximum power of the system can be attained by each output simultaneously or independently. The proposed inverter topology will perform the function of two single output inverters but with reduced component count which is a major advantage.

1.4 The Importance of The Thesis

The proposed inverter topology will perform the function of two single output inverters but with reduced component count which is a major advantage. The proposed two output series resonant inverter will provide the following advantages:

- Reduced losses
- Reduced inverter cost
- Reduced operational cost
- Increased efficiency
- Reduced component count

- Reduced volume and weight when compared to the single output inverter.

1.5 Limitation of Study

The absence of well-equipped laboratory prevents us from producing experimental results; also the simulation results are limited to the mathematical modelling used for the software design.

1.6 Overview of The Thesis

The body of the thesis is segmented into the following categories:

Chapter 1: Introduction, Thesis Problem, Aim of the Thesis, The importance of the Thesis, Overview of the Thesis

Chapter 2: Literature Review of Inverters

Chapter 3: Review of Resonant Converters

Chapter 4: Simulation Results

Chapter 5: Conclusion and Future Results

CHAPTER 2

LITERATURE REVIEW OF INVERTER

2.0 Introduction

This section of my research will review the various types of inverters with respect to the type of topologies, suitable control techniques and applications. Inverters are power electronic based circuit which are used to convert dc power into ac power. This is done by employing suitable topology composed of the right structure. The main components of inverters are semiconductor switches of appropriate power ratings.

2.1 Types of Inverters

Classification of inverters can be done with respect to different factors. Using the type of dc input as a reference then inverters are categorised into voltage source inverters (VSI) and current source inverters. With reference to the type of output voltage, inverters are mainly classified as multilevel inverters (MI). And finally with respect to the type of phase inverter are grouped into single-phase and three-phase categorise. The focus of this research will however focus on multiple inverters because the topology used for simulation falls under multilevel inverters. However consideration information of VSI and CSI will be provided.

2.2 VSI and CSI

Voltage source inverter are types of inverters in which the source or input power is derived directly from a voltage source such a battery, photovoltaic system, fuel cell and rectified ac source. VSI are the most common type of input for most inverters or converter because of several advantages such as: small inverter size, the load does not determine the nature of the output waveform, renewable energy compatibility and minimum inverter cost etc. however the voltage source has the following limitation: only buck functionality unless other topologies are included, EMI interference, output filter is needed to improve the quality of output waveform hence increased cost of inverter. To obtain current source inverters especially in the case of dc sources, a large inductor is connected in series with a dc VS. Some limitations of the current source are: has only boost functionality unless extra topologies are included to provide buck functions, open circuit is not desirable since it cause destruction of the switches, affected by EMI interferences (F. Z. Peng et al., 2002).

2.3 Multilevel Inverters (MI)

Multilevel inverters generate stepped voltages at the output by employing one or multiple dc sources with an appropriate converter structure and control technique. The stepped voltage or levels of output voltage should be three or more because the conventional 2-level topology is not considered as multilevel inverter. Base on the inverter structure, the H-Bridge inverter has received more research in academia and application in industry; most newly developed inverter structure can trace their roots to the H-Bridge structure. Single phase and three-phase are the most common types of phase with multilevel inverter applications. Multilevel inverters are generally classified into three groups:

- Neutral Point Clamped MI
- Flying Capacitor MI
- Cascaded Multilevel MI

2.3.1 Neutral point clamped (NPC) MI

The neutral point clamped MI which is also popularly referred to as diode clamped is a type of multilevel inverter in which several diodes are used in clamping the source voltage to specific capacitor values hence the number of the diodes required in this topology is extensively, the higher the levels of output voltage the higher the count of diodes required. Also higher levels comes with major limitations such as complex structure and complex controlling. However this topology requires only one dc source, the magnitude of the step output voltage is determined by the capacitors connected in series. The NPC topology was presented by (A. Nabae, H. Akagi et al., 1981) and after that several improvements have been made to the conventional topology in areas of structure and control techniques. Figure. 2.1 shows the circuit of the presented NPC by (A. Nabae, H. Akagi et al., 1981).

the structure is a three-phase system and it generates 3-step output voltage. Each phase is composed of four switches connected anti-parallel with a diode, also there are two blocking diodes per phase. The possible output voltages are +1/2Ed, 0 and -1/2Ed. The sources voltage is shared equally across the two capacitors hence we have:

$$V_{C1} = \frac{1}{2}E_d = V_{C2} = \frac{1}{2}E_d \tag{2.1}$$

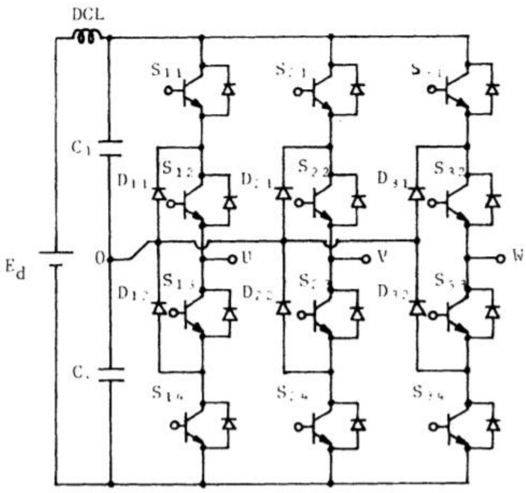

Figure. 2.1: 3-level NPC (A. Nabae, H. Akagi et al., 1981)

Apart from the conventional NPC topology which requires several diodes for voltage clamping purposes, new topologies of NPC have been developed which seeks to reduce the component count, especially the quantity of diodes, some of the popular developed topologies are the ANPC (Active NPC) and the T-Type NPC. In the ANPC as shown by Figure. 2.3, the clamping diodes are changed with switches and bidirectional switches are used to replace the switches in the ANPC to derive the T-Type NPC as represented by Figure. 2.4. The conventional NPC topology of a single phase system is shown by Figure. 2.2 (J. Holtz, P. Lammert et al., 1985). The following sections will review the various NPC topologies in terms of structure, applications and overall improvements.

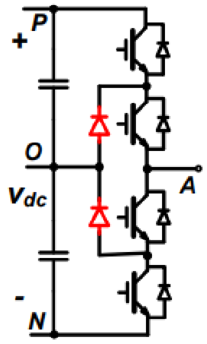

Figure. 2.2: NPC

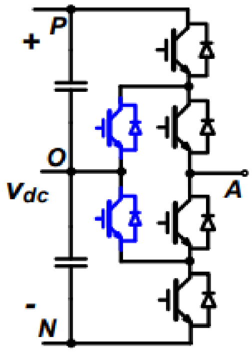

Figure. 2.3: ANPC

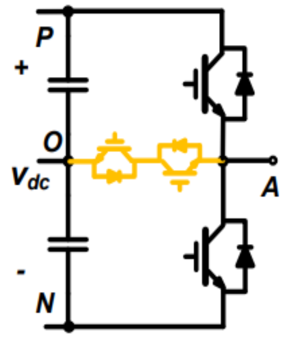

Figure. 2.4: T-type NPC

A review of hybrid clamped NPC topologies is extensively analysed in (Alian and Xiangning et al., 2006). In the reviewed topologies, a diode plus capacitor as clamping devices for a 5-level NPC inverter proposed by (Suh and Hyun, et al., 1997) is reviewed. The structure is composed eight switches with antiparallel diodes and clamping components of 12 diodes and 6 capacitors. Figure. 2.5 shows the circuit of the presented topology. The hybrid topology with same levels of output voltage is presented (Alian and Xiangning et al., 2006), the structure however reduces the clamping components of capacitors and diodes and replaces them with switch with antiparallel connected diodes. Four capacitors determine the magnitude of levels of output voltage, six switches, six diodes and three capacitors are the clamping components whiles the main switches are eight in number, the main advantage of this topology is that the clamping switches introduces control in the clamping of voltages whiles the topology with diodes does not offer any control in the voltage clamping. Figure. 2.6 show the hybrid 5-level NPC.

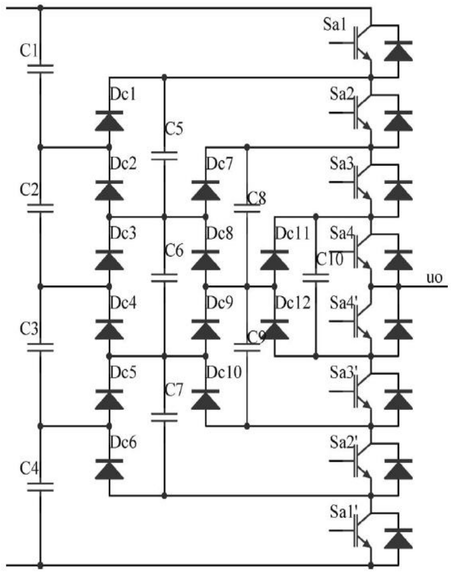

Figure. 2.5: 5-level NPC

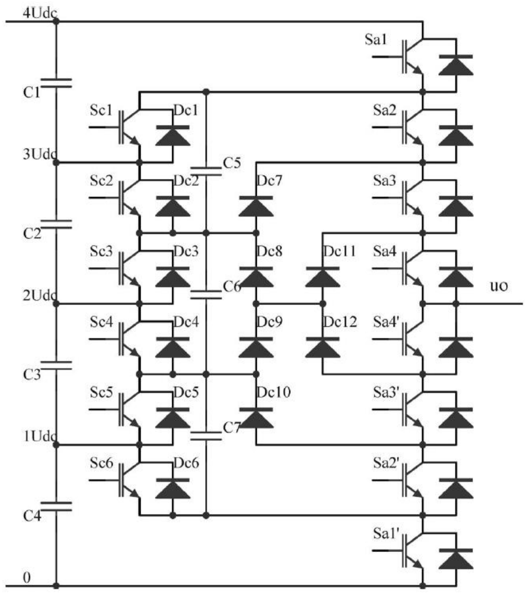

Figure. 2.6: Hybrid 5-level NPC

Figure. 2.7. Shows a symmetrical cascaded diode clamp multilevel inverter (F. Wu, B. Li, et al., 2017); it's a 9-level multilevel inverter. The concept of the cascaded NPC inverter is the same as cascaded H-bridge inverter. Two cells of NPC inverter are connected in series to develop the cascaded NPC inverter.

The voltage output of cell one and cell two are V_{ab}andV_{bc} and V_{ac} is the sum of outputs of cell one and cell two. To produce 2E at V_{ab}, switches T_{11}, T_{12}, T_{17} and T_{18} are put on (1). The same procedure is valid when 2E is required at V_{bc}. Cell one and two able to independently produce +2E, +E, 0 and –E, +2E. This means that to produce 4E at V_{ac}, V_{ab} should equal to 2E and V_{bc} should equal to 2E. Several switching patterns can be used to produce +4E, +3E, +2E, +E, 0, -E, -2E, -3E and -4E.

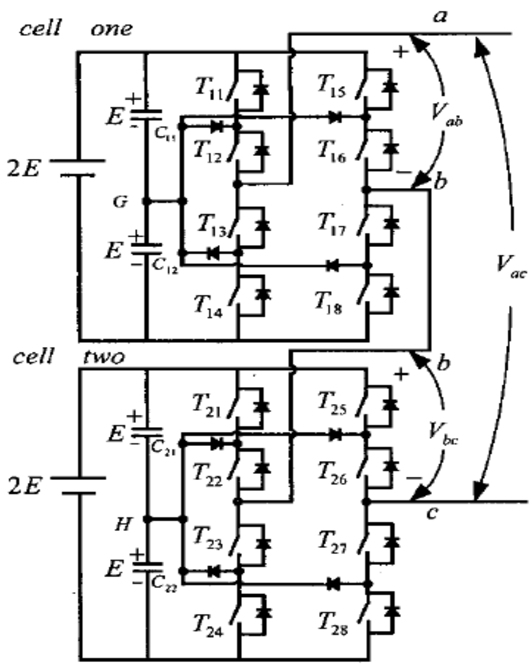

Figure. 2.7: Cascaded NPC inverter (F. Wu, B. Li, et al., 2017)

The zero current transition period of ANPC is extended in (L. Jin et al.,2009). This feature is possible by including resonant tank and helping switches; this introduces soft switching thereby reducing the switching losses and increasing the efficiency. The voltage stress experienced by all switches in the converter are minimized to half the source voltage. The circuit of the presented ANPC is shown by Figure. 2.8 and the commutation operation is shown by four states in Figure. 2.9 and Figure. 2.10. Detailed commutation of T_2 and D_3 are shown by Figure. 2.11.

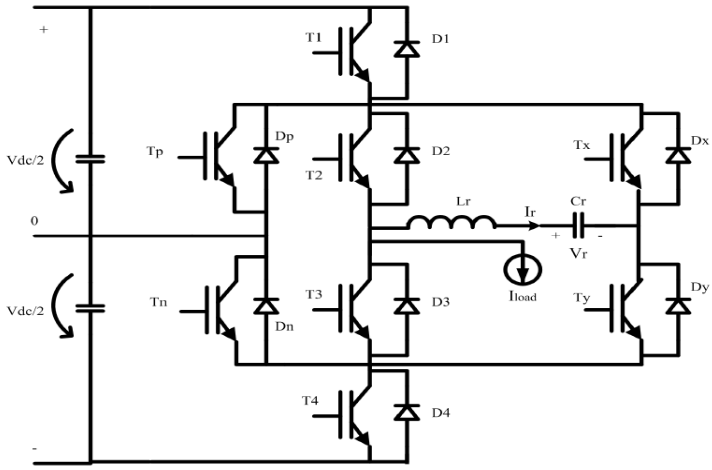

Figure. 2.8: 3-level ANPC (L. Jin, et al., 2009)

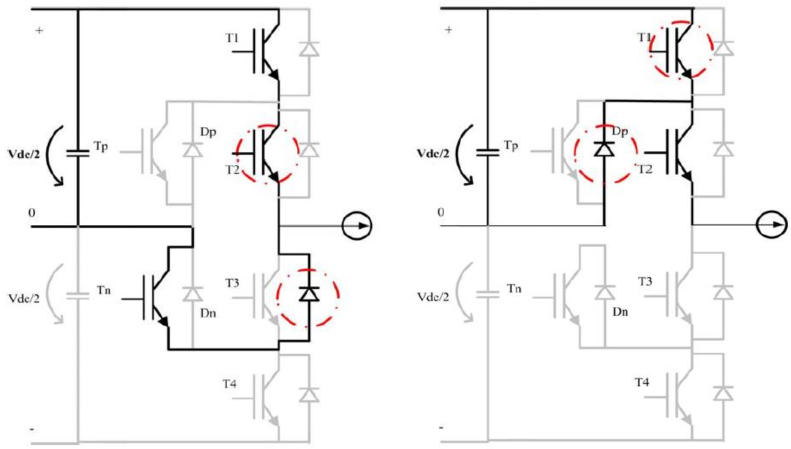

(a)Commutation between T2 and D3 (b)Commutation between T3 and D2

Figure. 2.9: Lower-path commutation (L. Jin, et al., 2009)

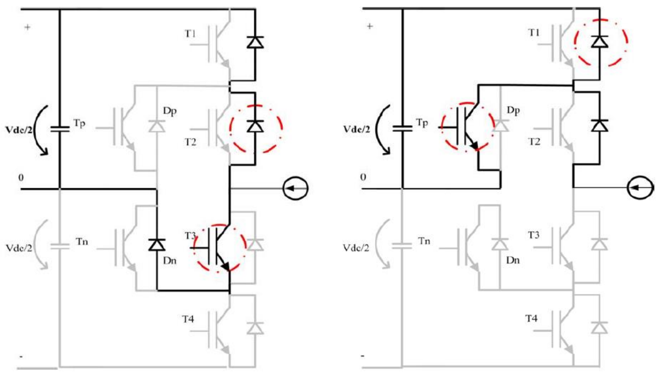

(a)Commutation between Tp and D1 (b)Commutation between T1 and Tp

Figure. 2.10: Upper-path commutation (L. Jin, et al., 2009)

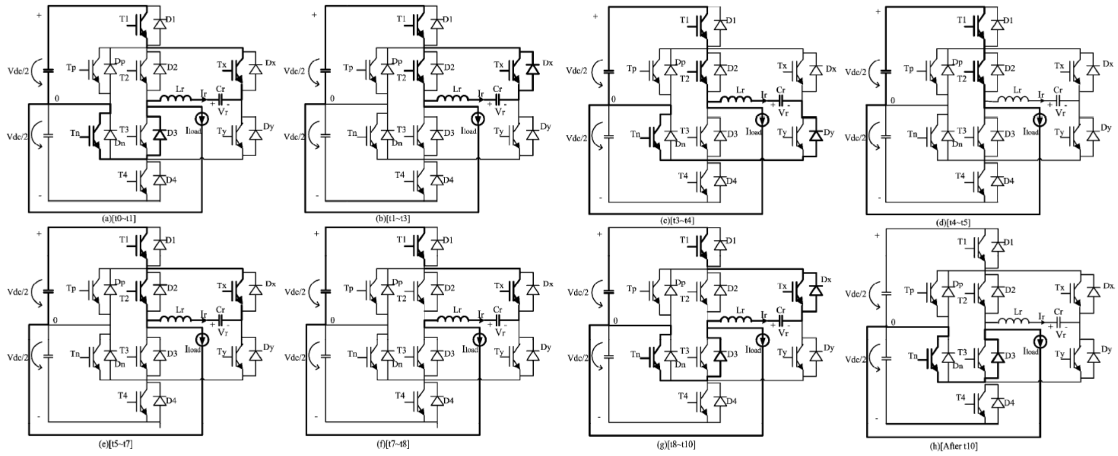

Figure. 2.11: Detailed diagrams for T_2 and D_3 (L. Jin, et al., 2009).

A family of NPC without transformer connection and derived from the H-Bridge structure, suitable for grid-tied photovoltaic system application are reviewed in (Li Zhang, Lanlan Feng et al., 2013). Figure. 2.12 is the main structure which is used to derive the structures of Figure. 2.13. Basically the direction of the switches are change to obtain positive and negative NPC structures respectively in Figure. 2.12a and Figure. 2.12b. InFigure. 2.13a, the positive and negative structures are combined to form the positive and negative NPC, similarly negative positive NPC topology is formed in Figure. 2.13b, dual positive NPC is formed in Figure. 2.13c and dual negative NPC is also formed in 2.13d.

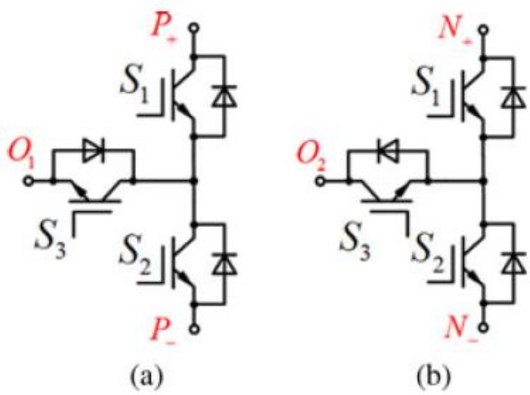

Figure. 2.12: P and N NPC topologies (Li Zhang, Lanlan Feng et al., 2013)

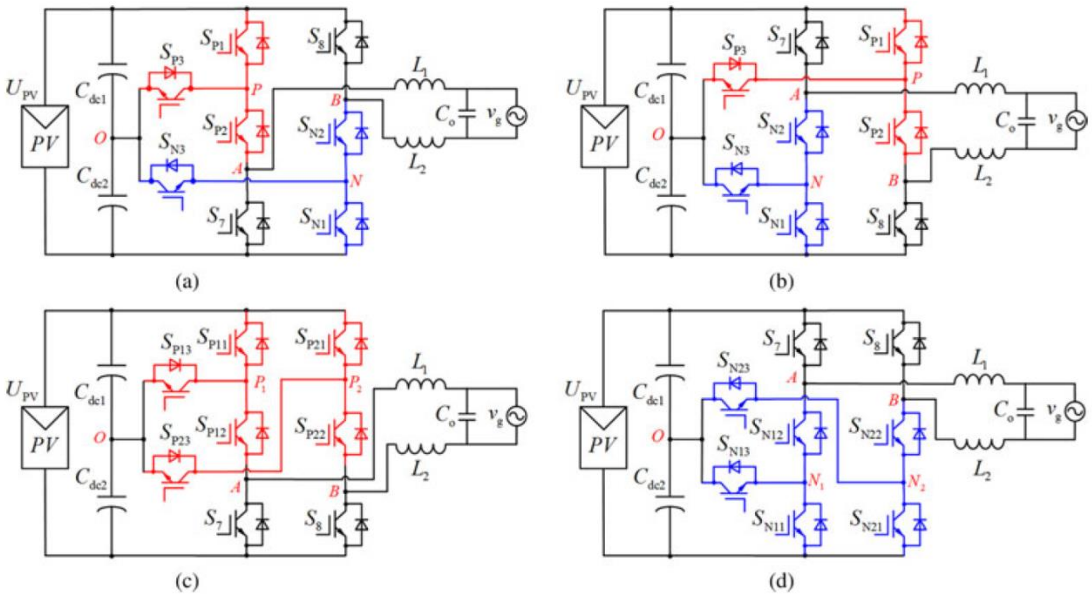

Figure. 2.13:P-N derived NPC topologies (Li Zhang, Lanlan Feng et al., 2013)

Two oH5 topologies of NPC is presented by (H. Xiao, S. Xie, et al.,2011). The circuit is composed of one dc source, two capacitors and six switches. There are no clamping diodes in this topology hence it belongs to the family of ANPC. The difference in the circuit of Figure. 2.14a and Figure. 12.14b is the direction of connection of the clamping switch.

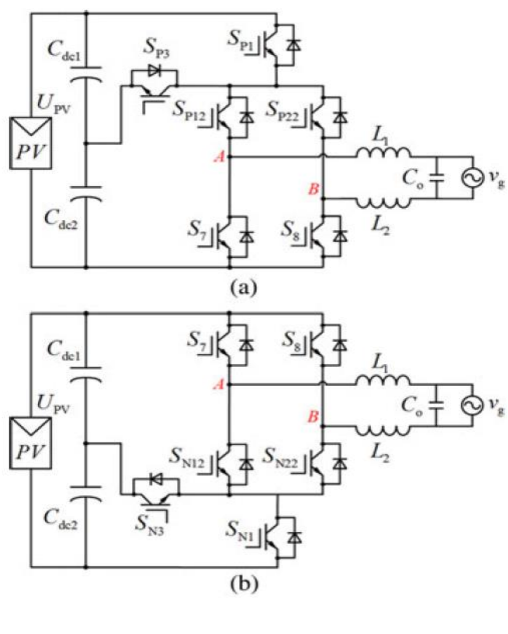

Figure. 2.14: 0H5 NPC (H. Xiao, S. Xie, et al.,2011).

The process of deriving the full bridge dc bypass inverter is extensively explained in (R. Gonzalez, J. Lopez, et al.,2007). The final circuit is composed one dc source, two capacitors and six switches without clamping diodes as shown by Figure. 2.15.

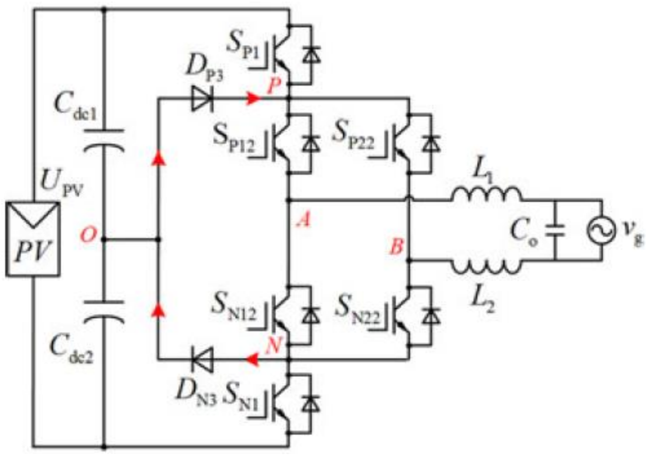

Figure. 2.15: Full HB-DC by pass inverter (R. Gonzalez, J. Lopez, et al.,2007).

A five level transistor clamped NPC topology based on the H-Bridge structure is presented in (Prakash Singh et al., 2012), presented topology utilizes eight unidirectional switches and 1 bidirectional switch, two capacitors and one dc source. When compared to other similar topologies, the presented topology boast of minimum component count. The circuit of the presented topology is shown by Figure. 2.16.

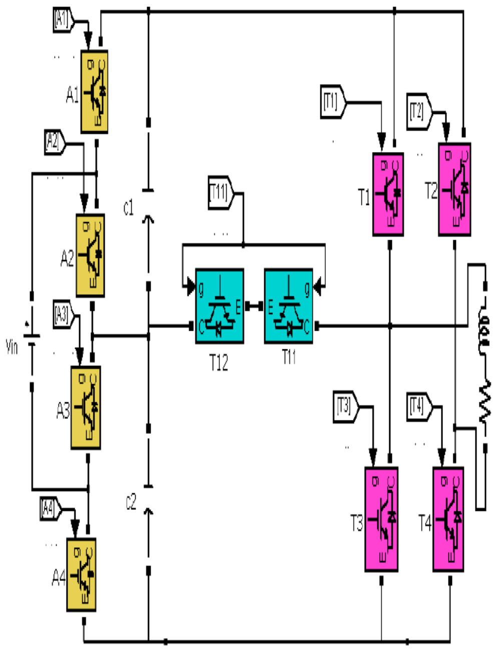

Figure. 2.16: Transistor clamped H-Bridge (Prakash Singh et al., 2012).

An impedance based NPC topology is presented by (Prakash Singh et al., 2012). The impedance structure when added to any converter provides numerous advantages such as buck-boost capabilities, reduced EMI interference and most important high boosting capabilities. The circuit of the presented ZS NPC is shown by Figure. 2.17. The impedance network is made up of symmetrical passive components; inductors and capacitors, the impedance network is placed between the input source and the main inverter circuit.

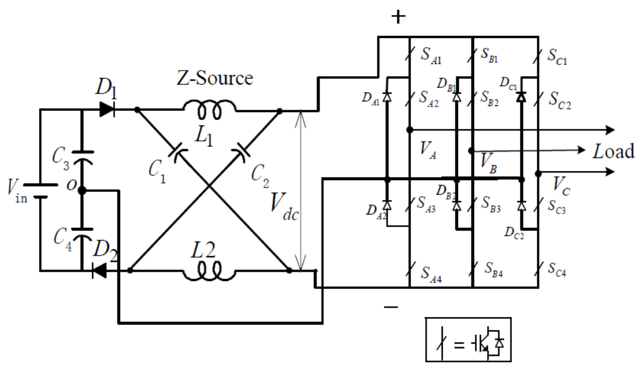

Figure. 2.17: ZS NPC (Prakash Singh et al., 2012).

Two other topologies of ZS NPC are presented, the cascaded topology and the 2 dc source topology which are represented by Figure.

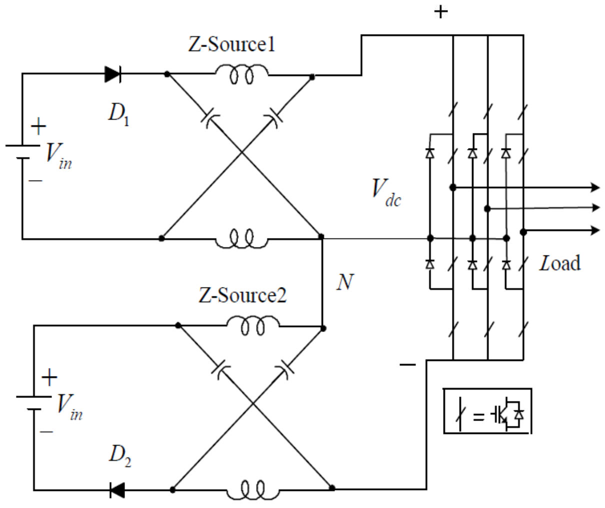

Figure. 2.18: Cascaded ZS NPC (Prakash Singh et al., 2012).

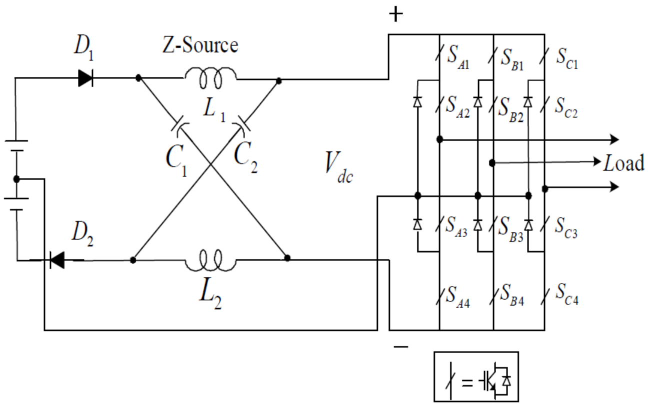

Figure. 2.19: Two dc source ZS NPC (Prakash Singh et al., 2012).

The mode of operation of the presented inverter is of two states; shoot through and non-shoot through. However the shoot through period is divided into two parts; the upper and the lower shoot through. In the period of shoot through, the impedance network has zero output voltage and the main inverter network is short circuit, also this period charges all the energy saving components hence provides the boosting phase of the inverter. The modes of operation are shown by Figure. 2.20.

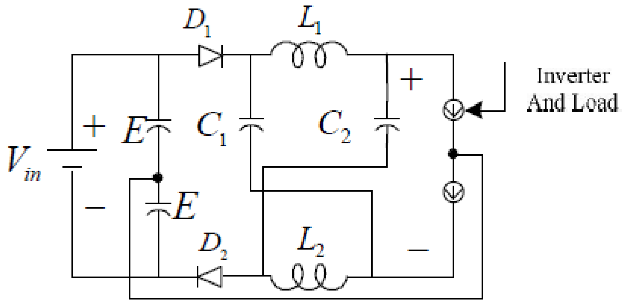

Figure. 2.20a: Non-shoot through mode (Prakash Singh et al., 2012).

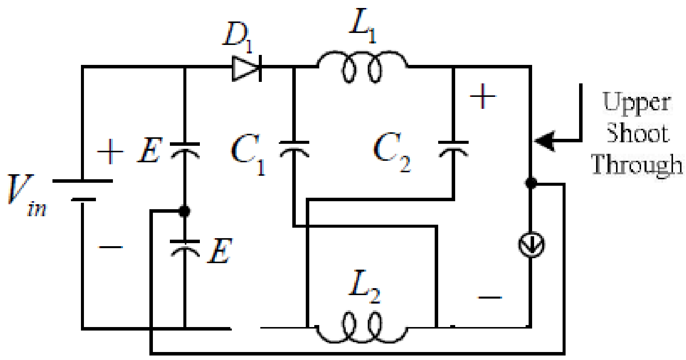

Figure. 2.20b: Upper shoot through mode (Prakash Singh et al., 2012).

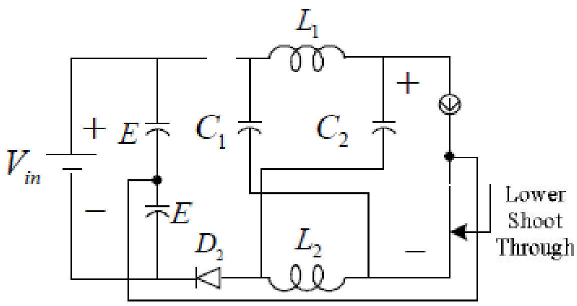

Figure. 2.20c: Lower-shoot through mode (Prakash Singh et al., 2012).

The inverter input voltage in non-shoot through mode is given:

$$V_i = \frac{2E}{1-\frac{T_O}{T}} \tag{2.2}$$

The inverter input voltage in shoot through mode is given:

$$V_i = \frac{E}{1-\frac{T_O}{T}} \quad (2.3)$$

The inverter output voltage is given by:

$$V_{ac} = [\frac{2E.M}{\sqrt{3}}] \quad (2.4)$$

A three-phase 5-level novel ANPC with minimum component count is presented in (Y.P. Siwakoti, et al., 2018). The active switch count is 6 with 2 of them not having anti-parallel diode connection, two capacitors and one dc input. These component count is for a phase hence the number of component will increase for the entire three phase system. Figure. 2.21 shows the circuit of the proposed three-phase system and Figure. 2.22 shows the circuit of a single phase for the same topology.

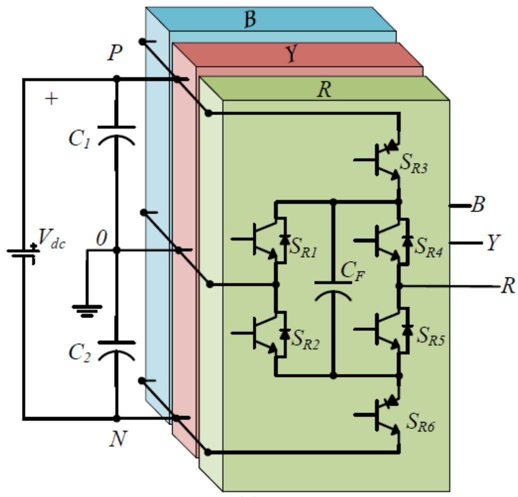

Figure. 2.21: Three-phase 5-level ANPC .

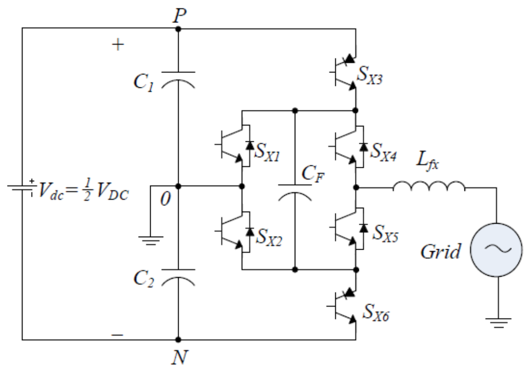

Figure. 2.22: Single-phase 5-level ANPC (Y. P. Siwakoti, et al., 2018).

2.3.2 Flying capacitor (FC) MI

In the flying capacitor (FC) topology, capacitors are used in voltage clamping and the step output voltage is determined by the magnitude of the capacitor voltage because one dc source is utilized and depending on the levels of output voltage, the dc source is divided by the series chain of capacitors connected in parallel with the dc source. The flying capacitor has some similarities with the NPC topology however clamping diodes are not desirable components in the FC topology. Some similarities between the FC and NPC topologies are that; the levels they can generate are limited because at higher levels, the structure becomes complex and also the control technique becomes cumbersome. A five level FC topology is shown in Figure. 2.23. One dc source, ten clamping capacitors and eight switches constitute the component count in the proposed topology. The magnitude of capacitor voltages reduces as the capacitors move further away from the dc source. The switching arrangement for Figure. 2.23 is given in Table 2.1.

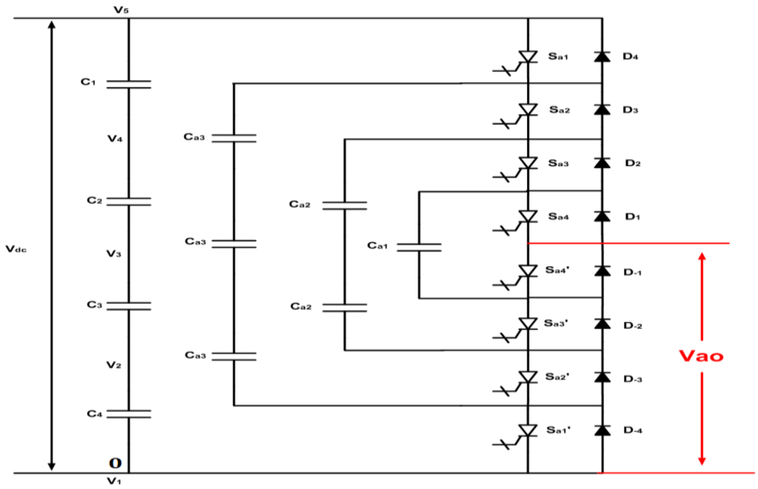

Figure. 2.23: Five level flying capacitor converter (G. Sinha, et al.,1997)

Table 2.1: Switching Pattern for 5-level flying capacitor converter

State	**Switches**							
	S_{a1}	S_{a2}	S_{a3}	S_{a4}	$S_{a'4}$	$S_{a'3}$	$S_{a'2}$	$S_{a'1}$
$V_5 = V_{dc}$	1	1	1	1	0	0	0	0
$V_4 = 3V_{dc}/4$	1	1	1	0	1	0	0	0
$V_3 = V_{dc}/2$	1	1	0	0	1	1	0	0
$V_2 = V_{dc}/4$	1	0	0	0	1	1	1	0
$V_1 = 0$	0	0	0	0	1	1	1	1

The advantages of the FC topology are enormous, some of which are(G. Sinha, et..1997):

- Harmonic reduction/elimination
- Cost saving because filters are not required
- No clamping diodes required
- Suitable for HV applications
- Reactive power compensation

The major limitation however is the large number of capacitors required. Also not suitable for higher levels of output voltage (J. S. Lai, et al.,1996). The following are some selected published papers on FC topologies.

A novel fault tolerant FC topology is presented in (Xiaomin and Familiant, et al.,2004), in the advent of single switch failure, the presented topology is able to provide the needed output voltage by short circuiting the faulty switch and reprogram the signal of the gate control. Hence the proposed inverter is capable of efficient functioning under single switch fault condition without compromising the quality of the converter. Figure. 2.24 shows the diagram of the proposed topology. It’s composed of one dc source, 2 capacitors and six unidirectional switches, it’s capable of generating four levels of output voltage. In the case of one switch being faulty, the mode of operation of the topology in Figure. 2.24 is segmented into six operational states as represented by Figure. 2.25.

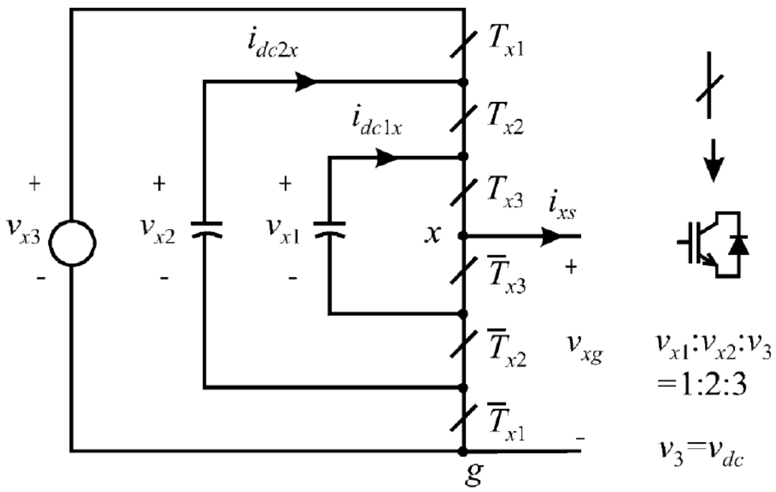

Figure. 2.24: Fault tolerant FC (Xiaomin and Familiant, et al.,2004)

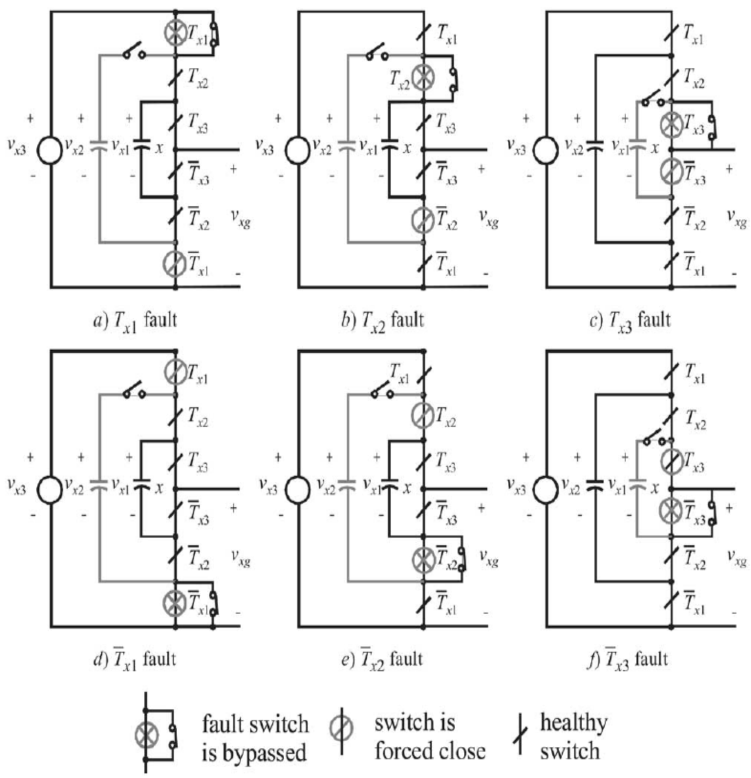

Figure. 2.25: Fault condition states(Xiaomin and Familiant, et al.,2004)

A three level FC topology with snubber circuit is presented in (K. In. Dong, N. Eui-Geun, et al.,2004). The snubber circuit of the under-land type hence constitute the basic snubber circuit. The proposed snubber circuit has more advantages when compared to the conventional snubber circuit, some the merits are: higher efficiency, reduced component, because of low over-voltage, the voltage stress is minimised hence the snubber losses is greatly reduced. Figure. 2.26 shows the conventional snubber circuit and Figure. 2.27 shows the proposed snubber based FC topology. The snubber circuit is composed diodes capacitors, inductors and resistors.

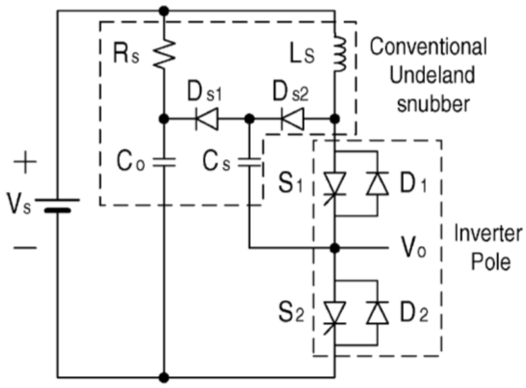

Figure. 2.26: Traditional under land snubber topology (K. In. Dong, N. Eui-Geun, 2004)

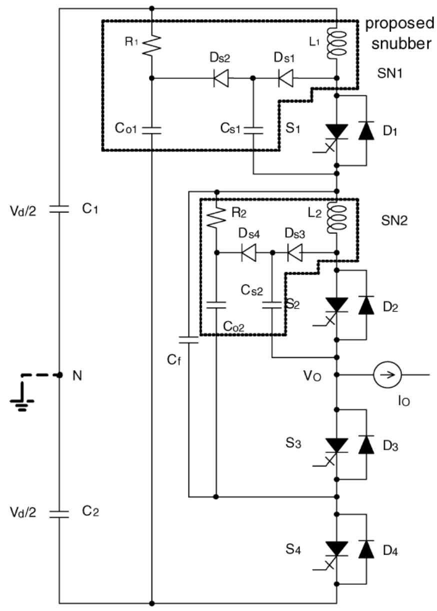

Figure. 2.27: Snubber based FC topology (K. In. Dong, N. Eui-Geun, 2004)

The switching state of the presented flying capacitor is such that only three levels of output voltage ($+v_d/2$, 0, $-v_d/2$) can be generated. Switches S_1 and S_2 are simultaneously gated on to generate the positive voltage whiles switches S_3 and S_4 are also simultaneously gated to produce negative voltage. To produce zero either S_1 and S_3 or S_2 and S_4 are gated on.

A novel topology of FC is presented by (P. Roshankumar, P. Rajeevan, et al.,2012). This topology combines two structure of FC and conventional H-Bridge hence the new topology is cascaded FC-HB converter. The three-phase topology is capable of generating 5 levels of voltage. Different magnitudes of pole voltages can be generated by utilizing the redundancy states. Balancing of the capacitor is also possible by virtue appropriate switching states. In advent of fault in the H-Bridge, the presented topology is capable of generating 3 levels from Fc structure. From the diagram below, the proposed topology uses one dc source for the whole system whiles each phase has two capacitors and eight switches.

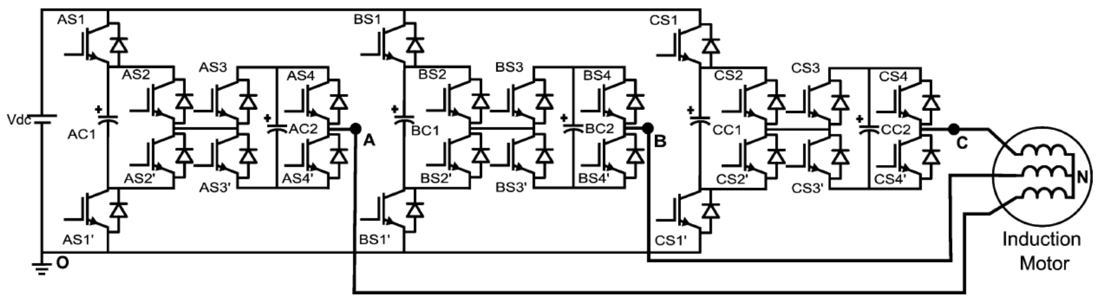

Figure. 2.28: Cascaded FC-HB converter (P. Roshankumar, P. Rajeevan, et al.,2012)

A novel topology of inverter based on two structures of flying capacitor and two level inverter is presented in (Q. A. Le, et al., 2016). This inverter is a hybrid topology and able to generate six levels. When compared to similar topologies, this converter utilizes minimum number of components to generate the same levels as other topologies. Minimum component count reduces the size, weight, volume and cost of the inverter and also increases the efficiency because the switching losses are minimised. When compared to conventional NPC and FC, the presented converter has minimum power loss. Figure. 2.29 shows the structure of the proposed converter, it's composed of flying capacitor structure and two two-level structures. There are six switches in FC structures, four switches in the two-level structures, four capacitors and one dc source.

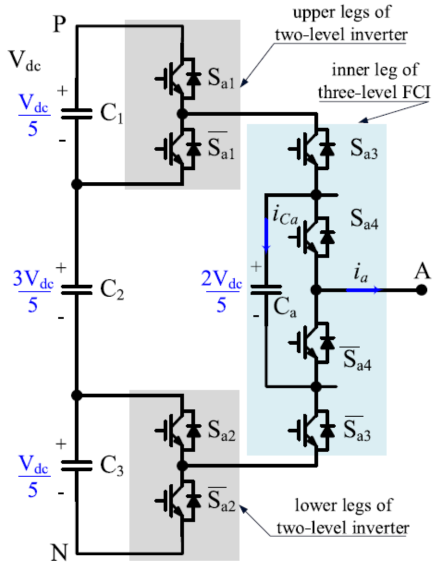

Figure. 2.29: Hybrid FC inverter(Q. A. Le, et al., 2016)

Table 2.2: Switching Pattern for 6-level Hybrid FC

State	S_{a1}	S_{a2}	S_{a3}	S_{a4}	V_{AN}	i_{Ca}
V_0	0	0	0	0	0	0
V_1	1	1	0	0	$V_{dc}/5$	0
V_2	0	0	0	1	$2V_{dc}/5$	$-i_a$
V_3	0	0	1	0	$2V_{dc}/5$	i_a
V_4	1	1	0	1	$3V_{dc}/5$	$-i_a$
V_5	1	1	1	0	$3V_{dc}/5$	$-i_a$
V_6	0	0	1	1	$4V_{dc}/5$	0
V_7	1	1	1	1	$V_{dc}/5$	0

A novel flying capacitor derived from the BMSC (Bridge-Modular-Switched-Capacitor) topology and capable of generating 5-levels is presented in(L. He, C. Cheng, et al.,2016). This converter boast of boosting capabilities provided by the dc-dc SC structure whiles the multilevel functionality is provided by the DC structure. Compared to the conventional cascaded MI, the presented inverter boast of minimum component count, reduced switching losses due to line voltage frequency modulation. Therefore the efficiency and power density of the presented inverter is greatly improved. Figure. 2.30 shows the circuit of the proposed converter. It's made up of twelve power switches, one dc source and four capacitors. The two state of operation of the SC structure is shown in Figure. 2.31 where Figure. 2.31a shows the positive cycle and Figure. 2.31b shows the negative cycle.

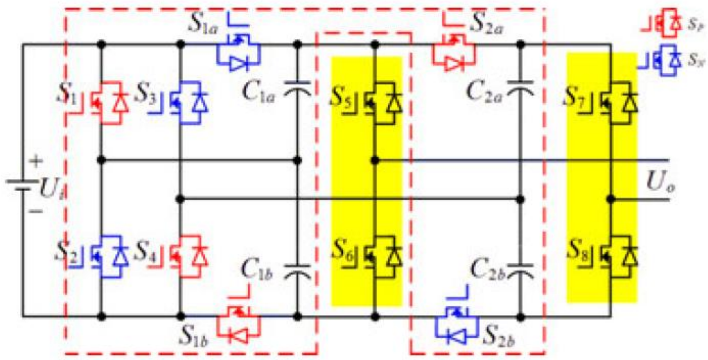

Figure. 2.30: FC-BMSC inverter (L. He, C. Cheng, et al.,2016).

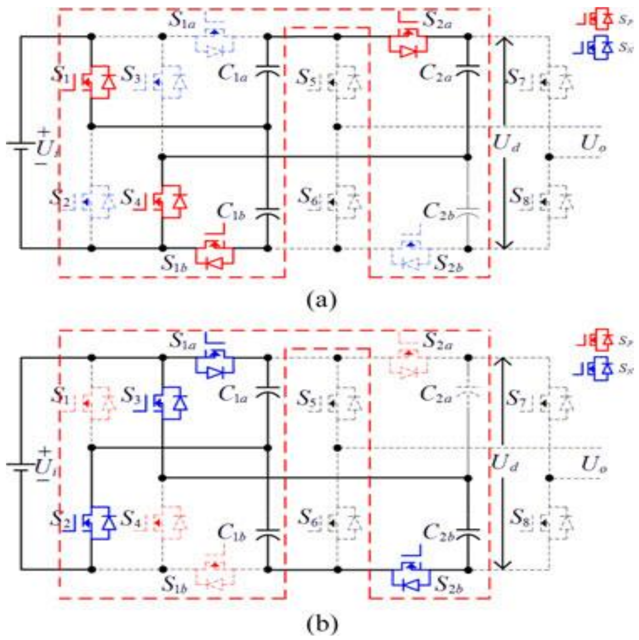

Figure. 2.31: FC structure operation (L. He, C. Cheng, et al.,2016).

2.3.3 Cascaded multilevel inverter

Cascaded multilevel inverter is a series connection of the basic unit or fundamental unit to form a multi-structure inverter thereby increasing the levels of the output of voltage. The most form of this topology is cascaded HB structure where the traditional H-Bridge structure is forms the basic unit used to form the desired multi-structure. Figure. 2.32 shows a cascaded HB structure where n-levels of output voltage are generated. Increasing the number of HB structures will increase the number stepped output voltage. The cascaded HB topology is a simple topology in terms of structure and control techniques when compared to the NPC and FC topologies; the cascaded topology does not require clamping diodes or clamping capacitors hence the component count in the cascaded HB topology is much lesser than FC and NPC (E. Babaei, S. H. Hosseini, et al., 2009). The cascaded NPC and cascaded FC are bedevilled large component count and complex structure. Modularity and simple structure is one major advantage of the cascaded HB topology. Each HB is composed of four switches and diagonal controlling of these switches will produce voltage of same magnitude but different polarity. One major advantage of the cascaded topology is that each basic unit requires separate dc source, however with increased penetration of renewable energy especially PV systems, this problem will be minimized. The relationship between the basic unit and the generated output levels is given by (2.5) where $\boldsymbol{n_l}$is the number generated output levels and $\boldsymbol{n_{HB}}$ is the number of H-Bridge structures used in the cascaded structure (S. M. Tenconi, et al., 1995).

$$n_l = 2n_{HB} + 1 \tag{2.5}$$

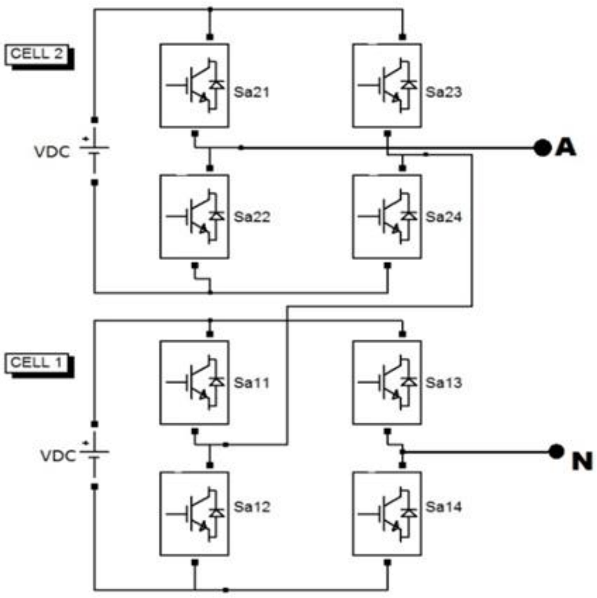

Figure. 2.32: Cascaded HB inverter (S. M. Tenconi, et al., 1995)

Table 2.3: Switching Pattern for 5-level cascaded converter (S. M. Tenconi, et al., 1995)

S_a21	S_a23	S_a22	S_a24	S_a11	S_a13	S_a12	S_a14	V_A	V_N	V_o
1	0	0	1	1	0	0	1	+E	+E	+2E
1	0	0	1	1	1	0	0	+E	0	+E
1	0	0	1	0	0	1	0	+E	0	+E
1	0	0	1	0	1	1	0	+E	-E	0
1	1	0	0	1	0	0	1	0	+E	+E
1	1	0	0	1	1	0	0	0	0	0
1	1	0	0	0	0	1	0	0	0	0
1	1	0	0	0	1	1	0	0	-E	-E
0	0	1	1	1	0	0	1	0	+E	+E
0	0	1	1	1	1	0	0	0	0	0
0	0	1	1	0	0	1	0	0	0	0
0	0	1	1	0	1	1	0	0	-E	-E
0	1	1	0	1	0	0	1	-E	+E	0
0	1	1	0	1	1	0	0	-E	0	-E
0	1	1	0	0	0	1	0	-E	0	-E
0	1	1	0	0	1	1	0	-E	-E	-2E

Table 2.3 shows the switching states for the 5-level cascaded topology of Figure. 2.32. With respect to dc voltage magnitude, the cascaded HB topology is segmented into two parts: symmetric CHB and asymmetric CHB. These two types of CHB topologies do not differ in structure but only in the value of the input dc voltage. In the case of the symmetric CHB, the magnitude of dc voltage for each of the H-Bridges are the same, for example the input voltage for Figure. 2.32 for cell I and cell 2 will be 10V each or 20V each or 30V each in the case of symmetric CHB. However in the case of asymmetric CHB, the magnitudes of input voltage differ. Using Figure. 2.32 as a case study, the input of cell 1 will be different for cell 2, so cell 1 can have 10V and cell 2 can have 30V. Also the asymmetric CHB can be further divided into two groups: trinary and binary topologies, further explanation of these topologies can be found in (E. Babaei, et al 2008-E. Babaei, S. Laali, 2014) Table 2.4 show the comparative difference between the types of cascaded HB.

The asymmetric topology is able to generate higher stepped output voltage when compared to the symmetric topology with the same component count. This translate to reduced cost for higher stepped voltage (E. Babaei, et al 2008).

The number of power switches required increases when there's the need to generate higher levels of output voltage. This will definitely affect the switching losses, will increase the cost of the converter and the number of driver circuits required. Irrespective of these limitation, the cascaded HB topology has received major application in industry and research in academia. The new ways been adopted by researchers is to minimize the component count in multilevel inverters whiles improving the efficiency; this features are been by improving the structure and the control methods which have been in practice over the years. Below are some selected papers of cascaded HB and cascaded MI.

A new topology of cascaded MI is presented in (E. Babaei, S. Laali, et al., 2015). This topology is derived from improving the structure of the conventional HB. Figure. 2.33 shows the fundamental structure which is composed of six bidirectional switches and two dc source. The proposed topology is capable of generating 5-levels of voltage. From the structure labelling's the output voltage generated is either the positive or negative polarity of V_1, V_1+V_2 and 0. The required voltage output waveform is shown by Figure. 2.34.

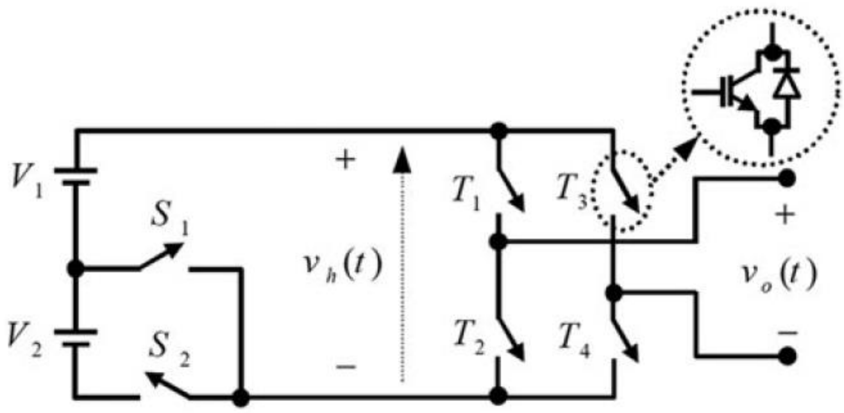

Figure. 2.33: Cascaded MI (E. Babaei, S. Laali, et al., 2015)

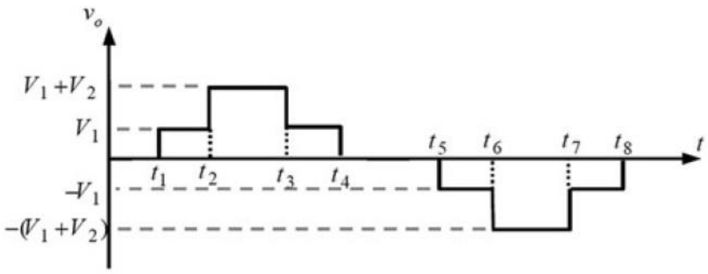

Figure. 2.34: Output voltage waveform (E. Babaei, S. Laali, et al., 2015)

The cascaded structure which is composed of series connection of the fundament structure of Figure. 2.33 is given in Figure. 2.35. Several algorithms have been proposed to generate the desired levels, for example in the first algorithm, the following mathematical equations are used where *x* stands for the number of fundamental structures in the cascaded unit.

$$Number\ of\ switches = 6x \quad (2.6)$$

$$Number\ of\ sources\ = 2x \quad (2.7)$$

$$Number\ of\ levels\ = 2^{x+1} - 3 \quad (2.8)$$

$$Maximum\ output\ voltage = (2^{x+1}\ - 2)V_{dc} \quad (2.9)$$

$$Blocking\ voltage = 10(2^{x} - 1)V_{dc} \quad (2.10)$$

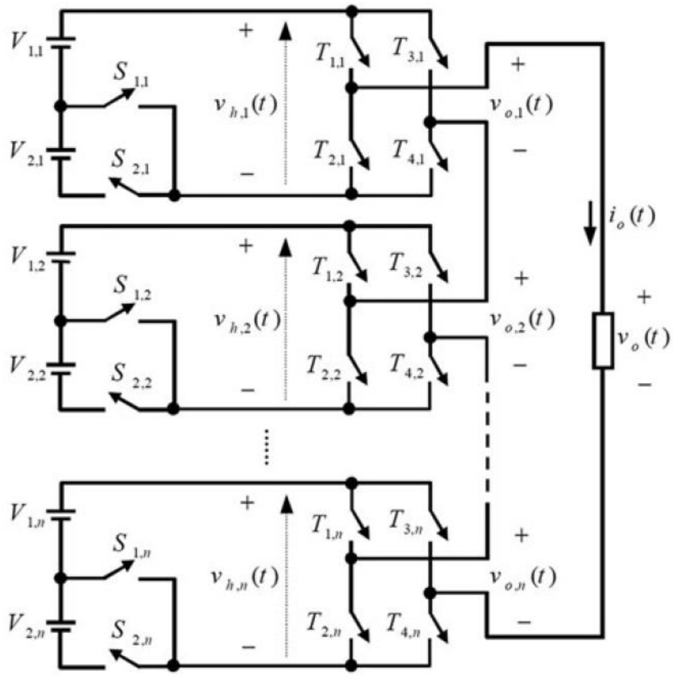

Figure. 2.35: Cascaded MI (E. Babaei, S. Laali, et al., 2015)

A novel cascaded MI is presented in (E. Babaei, S. Laali, S.Alilu., 2014) which is capable of generating 7-levels of voltage whiles employing minimum quantity of components. This inverter uses four unidirectional switches with respect to voltage and two dc sources. The control of the switches in this topology is similar to that of HB structure where diagonal control will generate the desired polarity of voltage. Including either the upper or lower switches will increase or sum the two dc sources. Figure. 2.36 shows the fundamental block whiles Figure. 2.37 shows the cascaded unit.

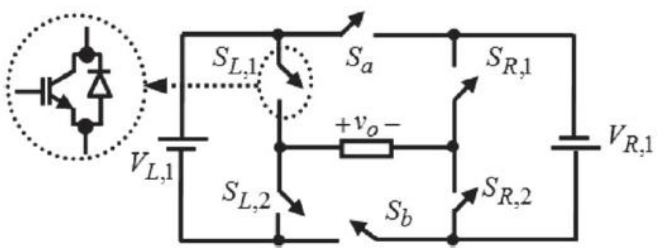

Figure. 2.36: Fundamental MI block (E. Babaei, S. Laali, S.Alilu., 2014).

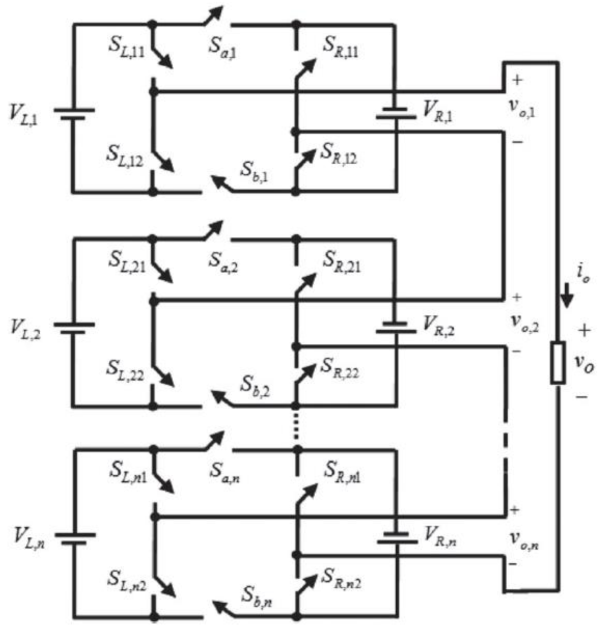

Figure. 2.37: Cascaded unit of MI (E. Babaei, S. Laali, S.Alilu., 2014).

A novel cascaded MI under symmetric and asymmetric investigation is presented in (M. F. Kangarlu, E. Babaei, et al.,2013). Under symmetric condition, the presented topology is suitable for charge balance control method and most importantly reducing the component count. The standing voltage of the topology is not maximised under this condition.

Also under asymmetric condition, the presented topology produces the highest number of levels and also maintains the standing voltage as in the case of symmetric state. Figure. 2.38 shows the common structure from which the cascaded topology is developed. The structure is made from a cross switched cell hence the topology is referred to crossed cell inverter.

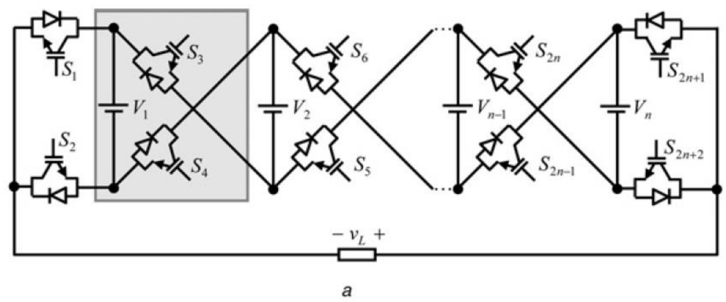

Figure. 2.38: Common structure (M. F.Kangarlu, E. Babaei, et al.,2013).

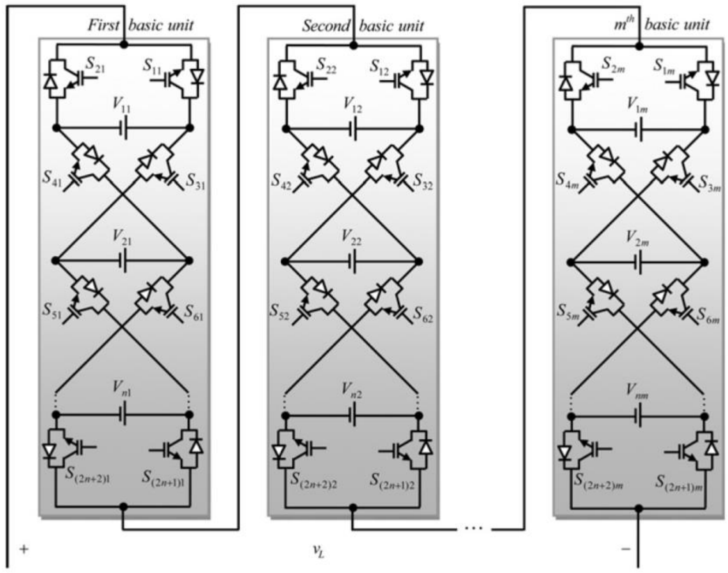

Figure. 2.39: Cascaded topology(M. F.Kangarlu, E. Babaei, et al.,2013).

The major parameters of the presented topology such as number of dc voltage, the levels generated, the standing voltage and required quantity of switches are given by:

$$N_{dc} = mn \tag{2.11}$$

$$N_{stepped} = 2mn + 1 \tag{2.12}$$

$$N_{swicthes} = 2mn + 2m \tag{2.13}$$

$$N_{standing} = 4mnV_d \tag{2.14}$$

A novel cascaded MI is presented in (E. Babaei, M. Farhadi, et al.,2012). This topology is investigated under both symmetric and asymmetric, also the component quantity is much less when compared to other traditional multilevel inverter topologies. A hybrid topology is also derived from this topology. The topology is composed of a new structure which is capable of generating only positive polarity output voltage hence the H-Bridge structure is added to provide the generation of negative polarity voltages. Figure. 2.40 andFigure. 2.41 shows the symmetric and asymmetric topologies.

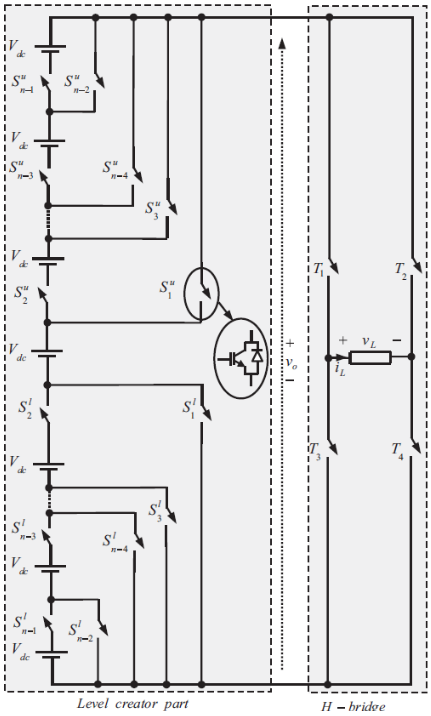

Figure. 2.40: Symmetric topology.

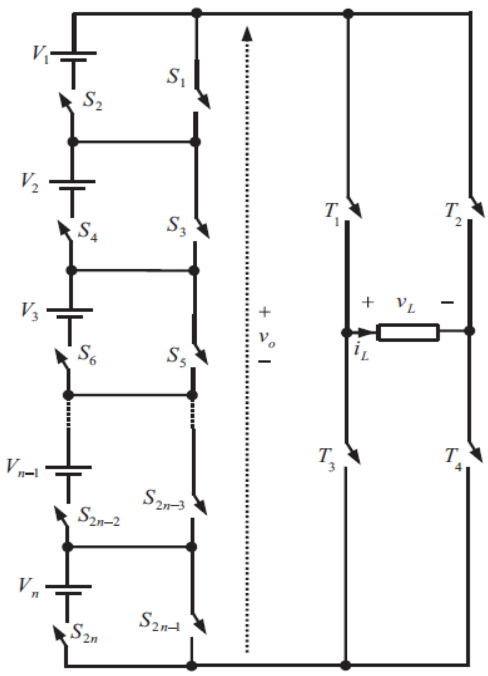

Figure. 2.41: Asymmetric topology.

2.4 Conclusion

Literature review of inverters is analysed in this section of the thesis. Classification of inverter are done with respect to any of the following or a combination of any of the followings categories: the type phase (single phase, two phase and three phase), the type of source (voltage or current) and finally the structure of the topology (NPC, Cascaded HB and FC). Selected topologies of multilevel inverters based on the traditional structures of NPC, Cascaded HB and FC are reviewed by analysing their power circuit and application.

CHAPTER 3

LITERATURE REVIEW OF RESONANT CONVERTERS

3.0 Introduction

Resonant converters (RC) provides the means by which high frequency switching of power electronic converter are possible without any major limitations. Applying resonant switching in high frequency based inverter or power conversion topologies provides the following advantages: minimum inverter size, minimum weight and reduced power loss. Basically resonant converters provide the states where switching occurs when there's zero voltage or zero current across the switches hence losses due to switching is large minimized.

High frequency switching of converters provides several advantages such better quality output waveforms, reduces the size of capacitors and inductors hence reduce converter size and cost and finally sometimes eliminates the need for filters. However this state of high frequency switching has such disadvantages such as maximum switching losses which translate to reduced efficiency.

To eliminate or reduce losses caused by switching in high frequencies, several techniques such as application of snubber circuits. This method however has some limitation which is increased losses (initial problem that we are trying to resolve) and dissipation of power. To best explain the issue with switching losses, let's analyze the Figures below.

Figure. 3.1 shows the half bridge of an H–Bridge whereI_o is the output current of an inductive load. The waveform of the voltage and current components in a linearized state is represented by Figure. 3.2. These waveforms occur during the switching states of the semiconductors switches, the turn-off current and voltage values are shown in the first section whiles the turn-on values for the voltage and current are shown in the second section. Finally Figure. 3.3 shows the graph for both states of switching, this graph shows the switching power losses is high when no protective technique is applied.

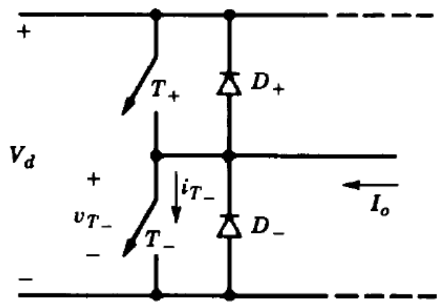

Figure. 3.1: Half H-Bridge (Mohan N, Undeland T.M, et al., 1995)

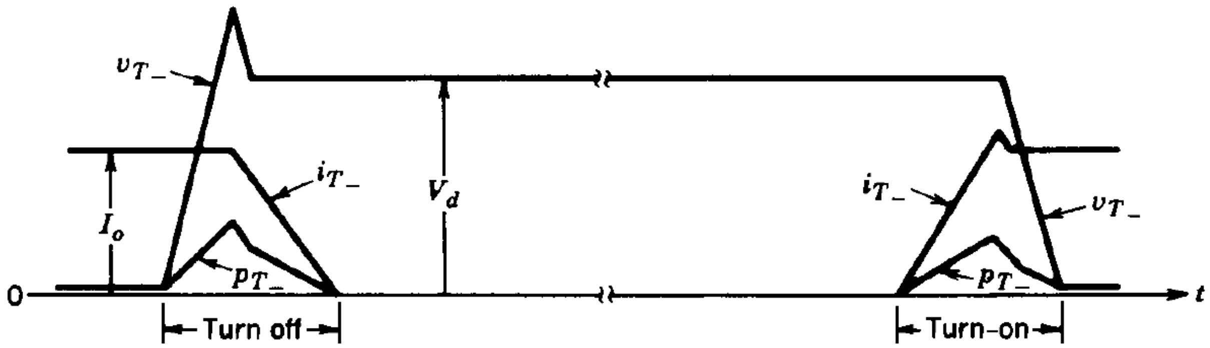

Figure. 3.2: Turn on and turn off mode of the half H-Bridge(Mohan N, Undeland T.M, et al., 1995).

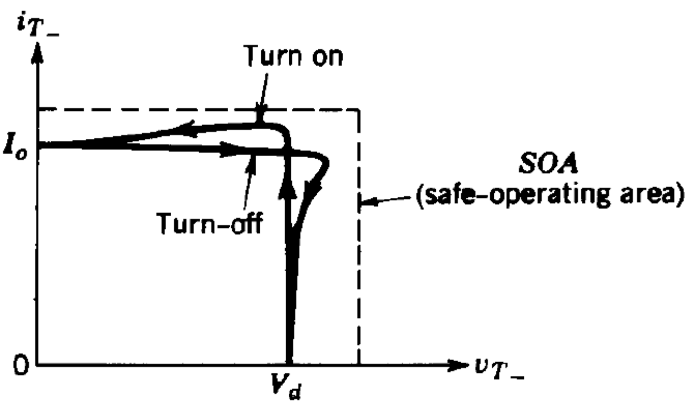

Figure. 3.3: Switching state curve (Mohan N, Undeland T.M, et al., 1995).

High switching frequencies in kilo-hertz, megahertz etc. have impactful advantages on the overall converter performance. This is because high switching frequencies will minimize the size of the filter components, minimize the weight and size of the transformer or eliminate the need transformer. Before applying such high frequencies, the limitation associated with it such as voltage stress, switching losses and EMI interferences needs to be resolved.

One solution for resolving the switching stress is to apply snubber circuit composed of passive and active components of resistors, capacitors and diodes. The snubber circuit is connected in parallel or series to the power switch. Two types of snubber circuits are connected across each switch; turn-on and turn-off snubber circuits. Figure. 3.4 shows the half H-Bridge switches with snubber circuits and the graph of the turn-on and turn-off (switching state) when snubber circuits are integrated into the converter is represented by Figure. 3.35.

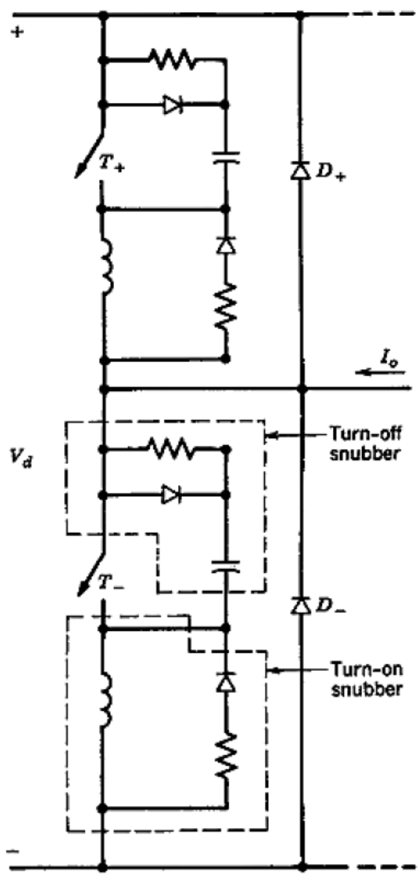

Figure. 3.4: H-Bridge with snubber circuit.

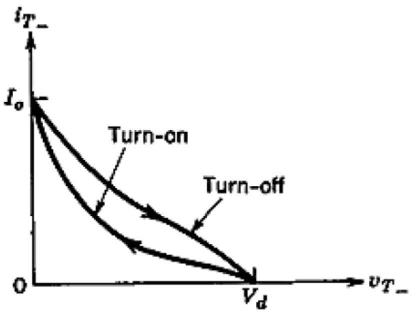

Figure. 3.5: Switching curve.

In other to overcome all the limitations associated with high switching frequencies, a proper converter topology and an appropriate switching mechanism can provide the state where switching occurs when the power switch voltage and current is at zero (0). Figure. 3.6 shows the desired state at which switching with high switching frequency should be done; zero current switching and or zero voltage switching.

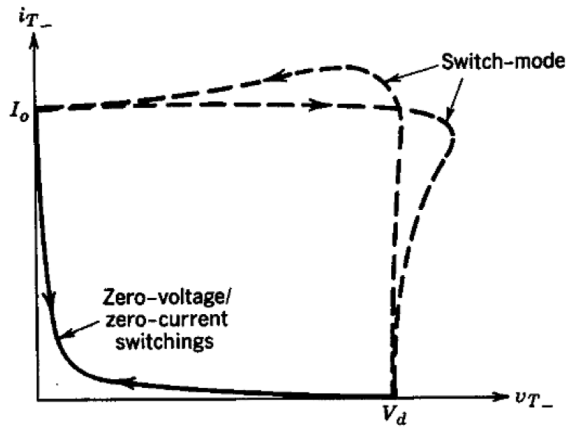

Figure. 3.6: ZVS/ZCS (Mohan N, Undeland T.M, et al., 1995).

3.1 Resonant Converters (RC) Classification

Resonant converter are groups of converter topologies and appropriate switching or control techniques which results in ZVS-ZCSconfigurations.

3.1.1 Load resonant converters

The load resonant converters are made up of various topologies of LC (inductor-capacitor) resonant tank (RT) topologies; oscillating or vibrating current and voltage which is caused by the LC component in the RT are connected to the load hence switching of the power switches at zero current and zero voltage are permissible. The load resonant converters can be connected to the load either in a series connection or in a parallel connection. The RT impedance controls the flow of power to the load whiles intern it's controlled by the switching frequency (f_s) and the output frequency (f_o). The load RC are sub divided into the following categories:

- Voltage Source Series-RC
- Current Source Parallel-RC
- Class E and Subclass E RC

Voltage source series-RC is also further divided into three groups:

- Series-load RC
- Parallel-load RC
- Hybrid RC

3.1.2 Resonant switch converters

In the switch topology, an LC is used to shape or form the switch current and voltage in other to achieve the desired zero voltage and zero current switching. Resonant switch converters are also classified as quasi resonant converters because two types of components or time intervals; resonant and non-resonant exist for each period of switching frequency. Resonant switch converters are classified into:

a. Resonant switch dc-dc converters:

- Zero current switching (ZCS) converters
- Zero voltage switching (ZVS) converters

b. Zero voltage switching clamped voltage(ZVS-CV) converters

3.1.3 Resonant DC link converters (RDCLC)

The conventional inverters work by utilizing a fixed dc input value to provide the needed ac output voltage by appropriate switching mechanism, however in the case of the RDCLC, LC resonant tank causes the input or source voltage to oscillate hence the input voltage remains at zero for a period of time to provide the duration of ZVS and ZCS.

3.1.3 High frequency resonant converters

The high frequency resonant converters are converters which have high frequency input and provides variable low frequency at the using ZV-ZC switching mechanism. In the resonant dc link converter the input voltage is made to wigwag via an inductor-capacitor resonance to achieve zero input voltage for a specific period hence ZV-ZC switching is obtained. The focus of my research is on load resonant converters hence review of published topologies will focus on the following types of resonant converters:

- Series-load RC
- Parallel-load RC
- Series-Parallel RC
- Hybrid RC

3.2 Series-Loaded RC (SL-RC) Topologies

The series RC circuit (underdamped) is shown by Figure. 3.7 where the input voltage is represented by V_d and the resonant tank components are L_r and C_r. The circuit equation are given by (3.1) and (3.2) using state variables i_L and VC at initial conditions of V_{C0} and I_{L0}. The output waveform is given by Figure. 3.8.

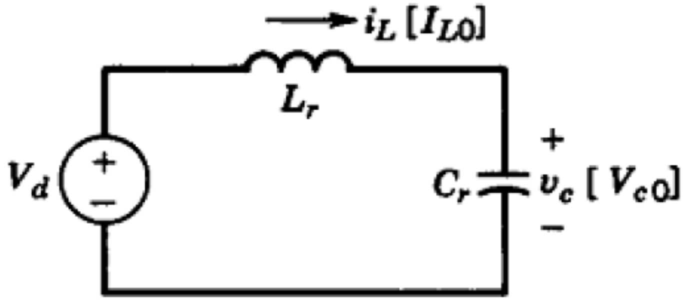

Figure. 3.7: Series RC

$$V_d = L_r \frac{di_L}{dt} + V_c \tag{3.1}$$

$$i_L = C_r \frac{dv_c}{dt} \tag{3.2}$$

$$\omega_0 = \frac{1}{\sqrt{L_r C_r}} \tag{3.3}$$

$$Z_0 = \frac{\sqrt{L_r}}{\sqrt{C_r}} \tag{3.4}$$

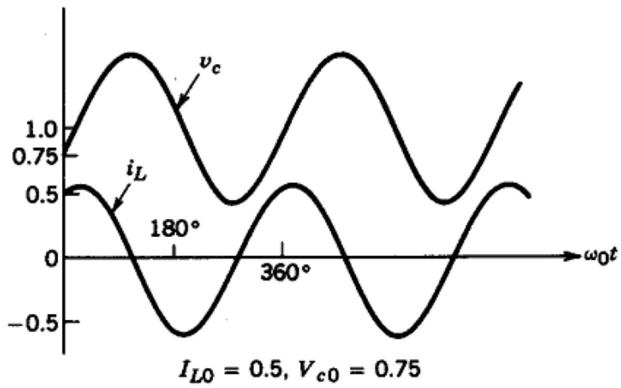

Figure. 3.8: Series RC output waveform

Some selected publications of the series resonant converters are review below with respect to converter structure, the type of control mechanism and the applications.

A new three-phase inverter with single stage power conversion is presented in (F. S. Hamdad, et al., 2004). which is operated with DCM (discontinues current mode) having a boost dc-dc section with a series resonant converter. The presented topology boast of the following features; soft switching, natural PF correction and isolation with HF transformer. The presented topology is thus named as BI-SRC (boost integrated SRC). Figure. 3.9 shows the circuit of the proposed converter, which is composed of four major part; the rectifier at the input side, the boost, the resonant tank coupled with the HF transformer and the output rectifier section.

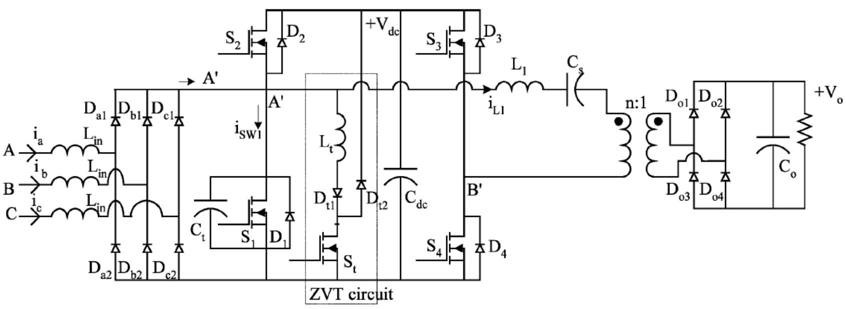

Figure. 3.9: BI-SRC

An improved series RC topology is presented in (Y. C. Chuang, Y. L. Ke, et al.,2009) which applied in renewable energy systems for charging of electric vehicle batteries efficiently. This presented charging system is a major improvements of the conventional charging systems which boast of 88% efficiency and it's operated under the continuous conduction mode. It's worth mentioning that the output of the proposed topology is connected with a voltage multiplier network. Resonant converters continue to receive much attention because of the several merits they offer; simple converter structure, minimum switching losses, simple control system and minimum EMI interference.

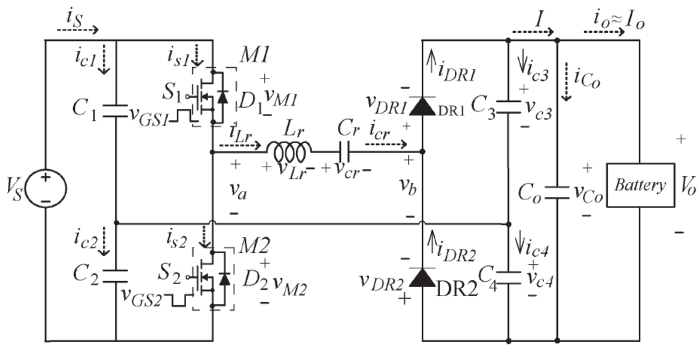

Figure. 3.10: Improved Half HB SRC

Figure. 3.10 represents the structure of the presented topology. It's composed of the half H-Bridge at the input section, a series RC and a voltage doubler output section with a rectifier circuit. The power switches of the half bridge is bidirectional in nature for reverse power flow, the input voltage is divided between the two series capacitors. Alternation of switching of the power switches at duty ratio of not more than 0.5. The four modes of operation of the switches are shown by Figure. 3.11 toFigure. 3.14. In each mode of operation, the input voltage becomes half of its magnitude and the output voltage becomes half of its magnitude.

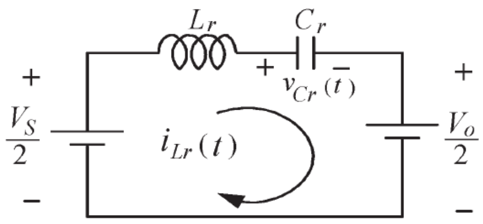

Figure. 3.11: Mode I operation

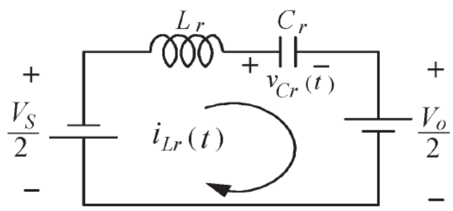

Figure. 3.12: Mode II operation

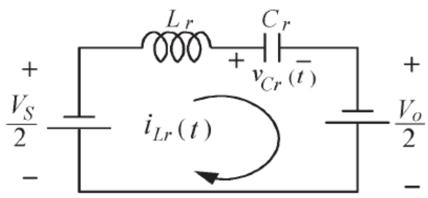

Figure. 3.13: Mode III operation

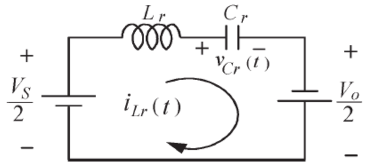

Figure. 3.14: Mode IV operation

The output voltage is given by:

$$V_O = V_S \frac{A-B}{A+B} \tag{3.5}$$

The boost factor is given by:

$$B = \left\{ -\left[\frac{V_S}{Z_o} + A - \frac{1}{Z_O}\left(\frac{V_S}{2} - V_{CO} - \frac{V_O}{2}\right)\right](1 - cos\alpha) + \frac{1}{Z_o}\left(\frac{V_o}{2} - V_{CO} - \frac{V_O}{2}\right) sin\alpha sin\beta \right\} \tag{3.6}$$

A dual bidirectional chopper (dc-dc) converter based series RC is presented in (Xiaodong Li, et al., 2010). This type of converter has received massive application in renewable systems due to two major merits which are: high power density and small converter size. The authors of this converter analyses this topology from two perspective: resistive load and VS load. ZV/ZC switching periods offer the operation of the power switches in wide voltage operation.

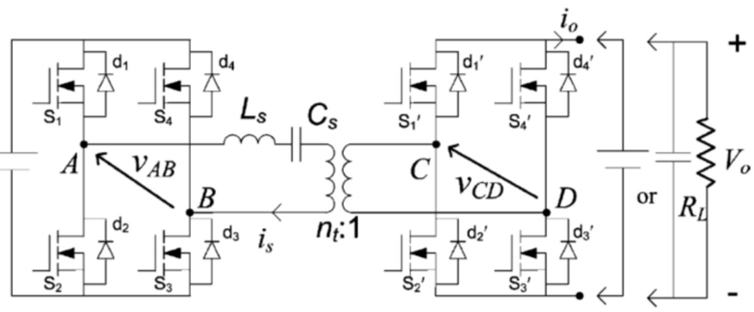

Figure. 3.15. Dual bidirectional SLRC

The proposed converter is represented by Figure. 3.15. It's made up of two H-Bridges sandwiched by resonant tank and a high frequency transformer. Bidirectional flow of power is possible due to the symmetric nature of the structure. The duty cycle operation is 0.5 and operates in CCM (continuous conduction mode) because the resonance frequency is much lesser than switching frequency. Figure. 3.16 shows the equivalent circuit of the proposed converter.

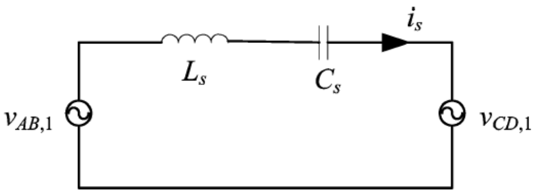

Figure. 3.16: Equivalent circuit

$$I_{ac} = I_O^1 \frac{\pi}{\sqrt{8cos\theta}} \tag{3.7}$$

$$P_O = E_o I_{ac} cos\theta \tag{3.8}$$

$$M = \frac{Z_{ac}}{Z_{ac}} + jX_s \tag{3.9}$$

$$M = \frac{8sin\varphi}{Q\pi^2(F - \frac{1}{F})} \tag{3.10}$$

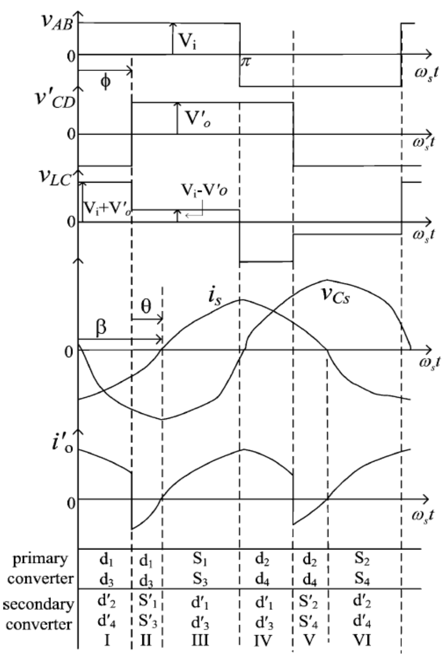

Figure (a) Charging waveform

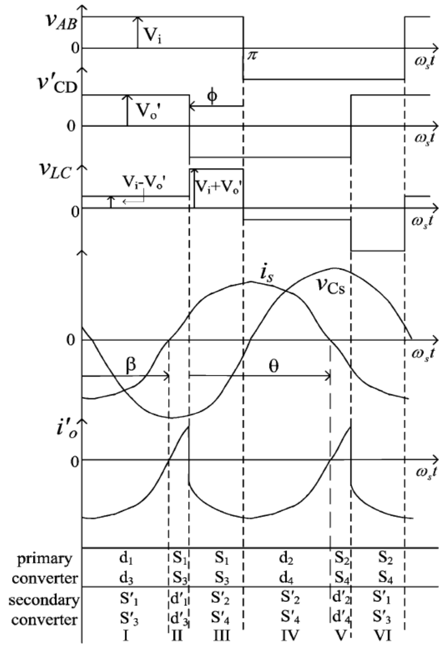

Figure (b) Discharging waveform

A novel three port converter derived from three H-Bridge structures is proposed for renewable energy applications. This converter is composed of three HB structures, resonant tanks and a transformer with three windings. Figure. 3.17 shows the topology of the converter. This converter controls the power flow between the various parts by utilizing HF link and single stage conversion. Bidirectional power flow is also possible between the source and the load. Inclusion of the resonant tank allows the switching of the semiconductor switches with high frequency which leads to a major reduction in the switching power loss values when compared to the same conventional topology with only an inductor. Also the efficiency values are large improved (H. Krishnaswami, et al., 2009).

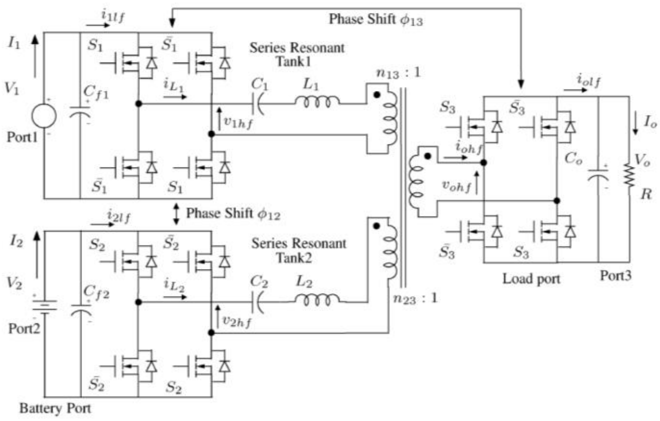

Figure. 3.17: 3-port SLRC

Figure. 3.17 shows the circuit of the presented topology, it's composed of two resonant tanks, and three H-Bridge structures and a transformer with three windings to interconnect the H-Bridges, also there are input and output filters.

A buck inverting converter with resonant converter is presented in (M. Jabbari, et al., 2010). The resonant converter is of LC nature and the converter structure is composed of half H-Bridge. As in the case of all resonant converters, soft switching of the power switches is provided hence the switching losses are reduced. To protect components in case of short circuit, the converter is automatically turned off and also the voltage gain is variable. Figure. 2.18 shows the topology and its modes of operation are shown by Figure. 3.19. The voltage gain is expressed mathematically by:

$$A = \sqrt{\frac{f_s . r}{f_r . \pi}} \tag{3.11}$$

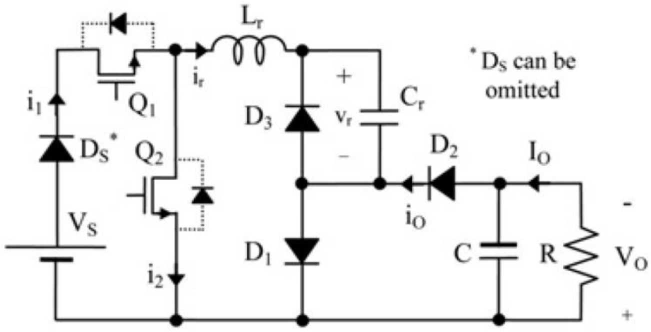

Figure. 3.18: Buck resonant converter

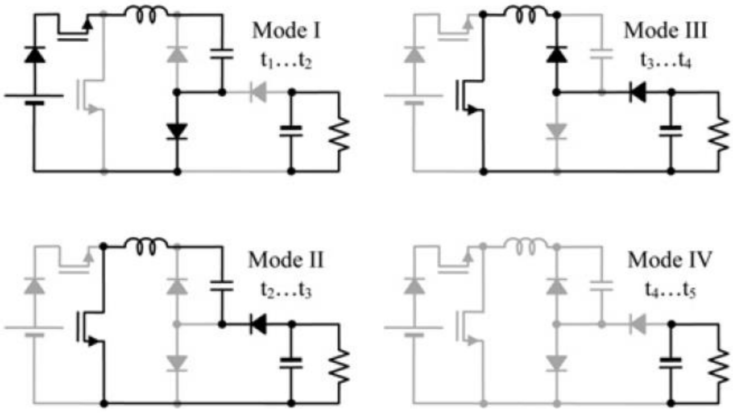

Figure. 3.19: Modes of operation

A novel control of full bridge series RC is presented in (Y. K. Lo, C.Y. Lin, et al.,2011). The control method utilized is the phase shifted PWM method. In this mode of control, two novel operation techniques are employed. The first being the resonant (series) state operation; control of the load (normal) via output voltage is done by varying the switching frequency. The second method is using the fixed frequency, where the output voltage is controlled at light loads by varying the duty cycle. The presented converter boast of high efficiency for variety of load conditions. Figure. 3.20a shows the presented converter with H-Bridge at the primary side, and rectifier circuit at the output or secondary side, the series resonant converter and the transformer is sandwiched between them.

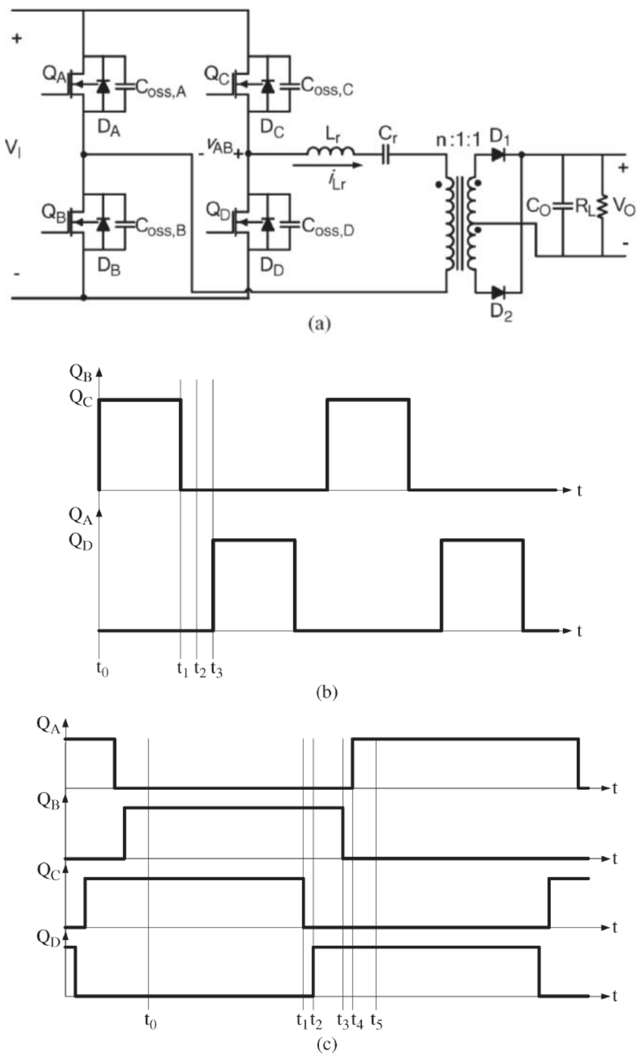

Figure.3.20 : a) Presented converter

b) Switching frequency PWM

c) Duty PWM

An induction cooking converter built from half H-Bridge is presented in(I. Millan, J. M. Burdio, et al.,2011). The presented topology seeks to improve the heating capabilities of both ferromagnetic and non-ferromagnetic materials by using the selective harmonic technique. The modes of operation of the presented topology is segmented into two parts or states:

- First selective-harmonic technique

- Third selective-harmonic technique

Figure. 3.21 shows the structure of the presented topology which is composed of the half bridge, the resonant tank and the output capacitors.

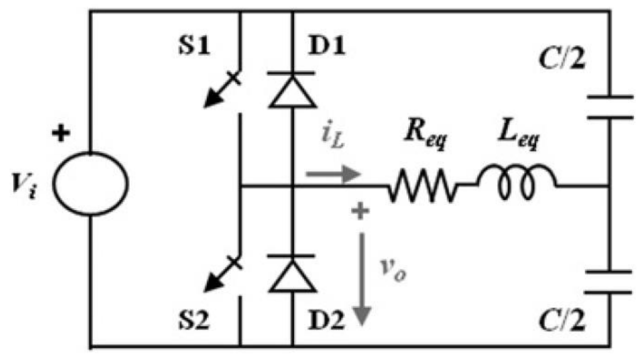

Figure. 3.21: Half HB SRC

$$C = \frac{1}{4\pi^2 f_s^2 L_{eq}} \tag{3.12}$$

$$f_o = \frac{1}{2\pi\sqrt{L_{eq}C}} \tag{3.13}$$

$$f_s = \frac{1}{2\pi h\sqrt{L_{eq}C}} \tag{3.14}$$

A novel isolated LLC series RC is presented in (S. M. Showybul, et al., 2017). The proposed converter is a dc-dc converter and it's suitable for wide input voltage applications. The appropriate control method applied is the frequency adaptive PS-PWM. The control technique enables high boosting capabilities and zero voltage switching; irrespective of the load state. The input side of the topology is made up of cascaded Half-Bridge structure; this provides minimum switching stress on the components of the input side. Figure. 3.22 shows the circuit of the proposed converter. The resonant tank is connected to an HFT, transformer saturation is prevented by utilizing capacitor C_r (resonant capacitor) to absorb the dc component of the ac voltage. The switch stress is minimized to half the source voltage. High capacitor value is chosen for the output section in other to eliminate ripples. The voltage gain is given by:

$$G = \frac{1}{\sqrt{\left\{\left(1+K-\frac{K}{F^2}\right)-\left[\frac{Q(F^2-1)}{F}\, x\left(\frac{FK+F-\frac{K}{F}}{Q(F^2-1)}-cot\varphi\right)\right]\right\}^2+\left\{\frac{Q(F^2-1)}{F}\right\}}} \tag{3.15}$$

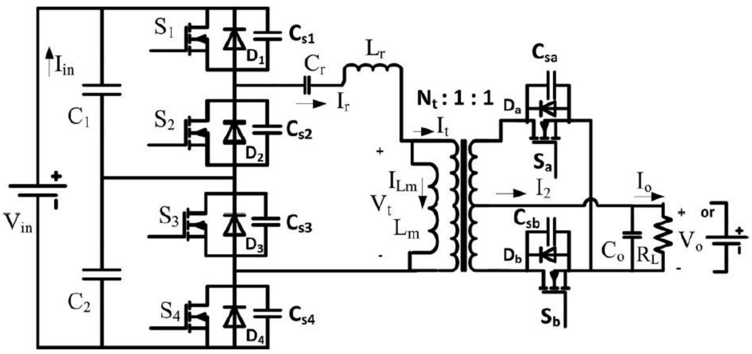

Figure. 3.22: Novel LLC converter(S. M. Showybul, et al., 2017).

Another topology of the series resonant tank is the capacitor-load parallel connection; this simply means that the capacitor of the resonant tank is connected in parallel with the load. Figure. 3.23 andFigure. 3.24 shows circuit and the output waveforms respectively.

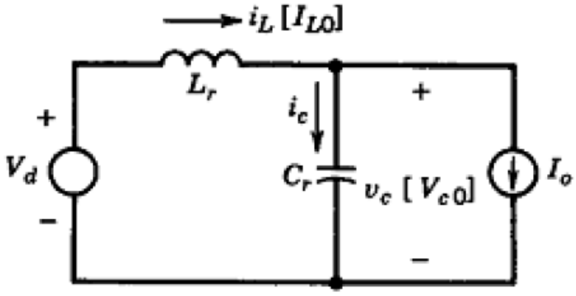

Figure. 3.23: Parallel capacitor-load SLRC

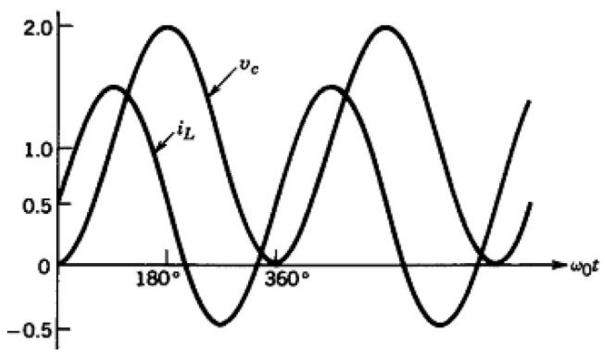

Figure. 3.24: Output waveform

From Figure. 3.23, the input and output parameters are V_d and I_o which are *dc* parameters. Using the following initial conditions will yield the following expressions:

$$V_C = -L_r \frac{di_L}{dt} + V_d \tag{3.16}$$

$$I_O = -i_C + i_L \tag{3.17}$$

$$i_C = -\frac{C_r L_r d^2 i_L}{dt^2} \tag{3.18}$$

$$I_L(t) = \frac{V_d sin\omega_0(t-t_o)}{Z_o} + I_O \tag{3.19}$$

$$V_c(t) = V_d[1 - cos\omega_o(t - t_o)] \tag{3.20}$$

3.3 Parallel-Loaded RC (SL-RC) Topologies

The parallel-loaded RC circuit (underdamped) is shown by Figure. 3.25where the input voltage is represented by I_d and the resonant tank components are $L_r$and C_r. The circuit equation are given by (3.19) to(3.22) using state variables $i_L$and v_c at initial conditions of V_{C0} and I_{L0}. The output waveform is given by Figure. 3.25.

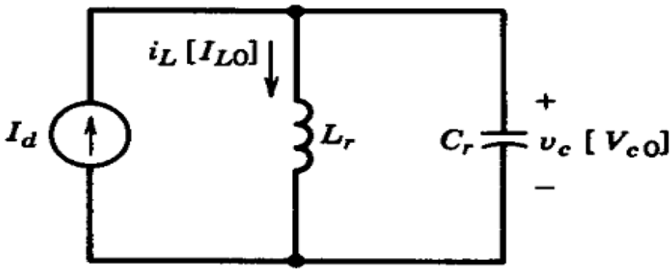

Figure. 3.25: Parallel RC

$$I_d = i_L + c_r \frac{dv_c}{dt} \quad (3.21)$$

$$v_c = L_r \frac{di_L}{dt} \quad (3.22)$$

$$\omega_o = \frac{1}{\sqrt{L_r C_r}} \quad (3.23)$$

$$Z_o = \sqrt{\frac{L_r}{C_r}} \quad (3.24)$$

A half H-Bridge which has been modified and with asymmetric features is presented in (Neilor C. Dal Pont, et al., 2019). The dc offset current in the transformer has been eliminated. The method of control of this inverter is similar to the traditional H-Bridge topology where a sustained frequency and asymmetric PWM technique is utilized. To prevent the flow of dc component of the inverter output to the transformer, a voltage doubler is connected to the transformers output. The resonant tank of parallel connection is fixed between the inverter output and the transformer input. Figure. 3.26 shows the circuit of the presented topology. Two switches of the inverter have different conduction times, switch S1 operates during the time period of DT_s whiles the remaining switch S2 conducts during the time period of $T_s(1\text{-}D)$ which the complementary mode of conduction. The voltage multiplier increases the magnitude of the output voltage hence minimum turns ratio is required in the transformer. The parallel resonant tank provides the ZV-ZC switching. The equivalent circuit of the six modes of operating the proposed topology is provided in Figure. 3.27.

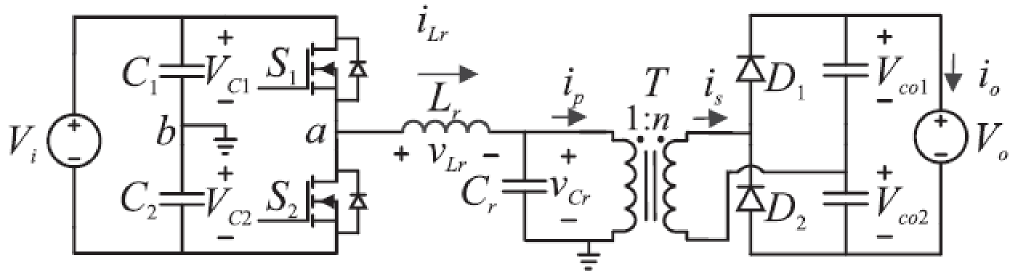

Figure. 3.26: Modified HB PL-RC (Neilor C. Dal Pont, et al., 2019).

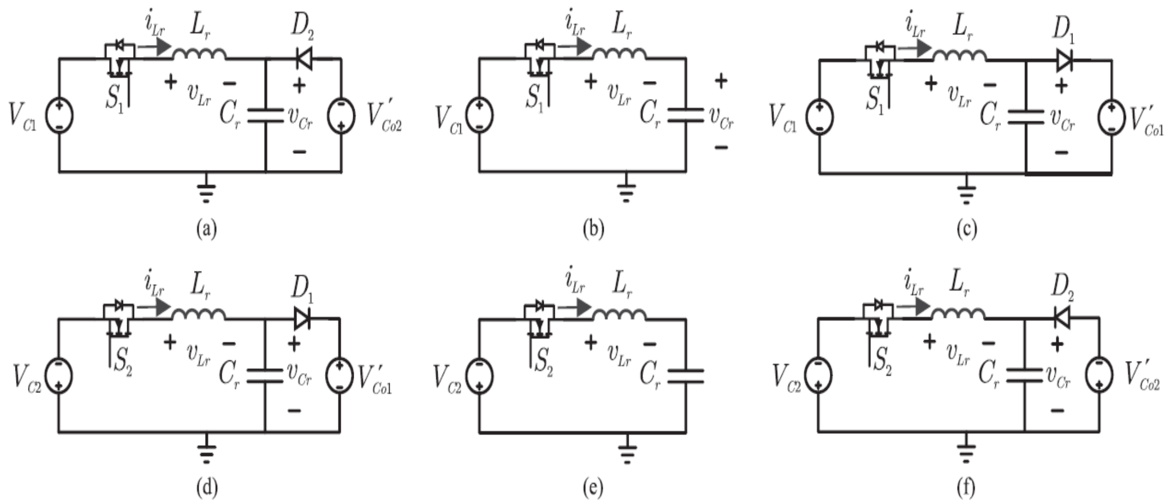

Figure. 3.27: Six modes of equivalent circuit (Neilor C. Dal Pont, et al., 2019)

A novel phase controlled PRC is presented in (M. K. Kazimierczuk, et al., 1993). This converter is derived from the parallel connections of equal parallel resonant tank output loads. The output voltage amplitude for the new converter is varied by phase shifting the signals (drive) of the two converter structures. The presented topology has better performance against EMI interferences. Also the output voltage can be from the states of full load to the state of no load. The structure of the proposed converter is given by Figure. 3.28. The two converters are located at the input and output sections and between them is the parallel connected resonant tank. The converters are half H-Bridges and the switches are unidirectional types.

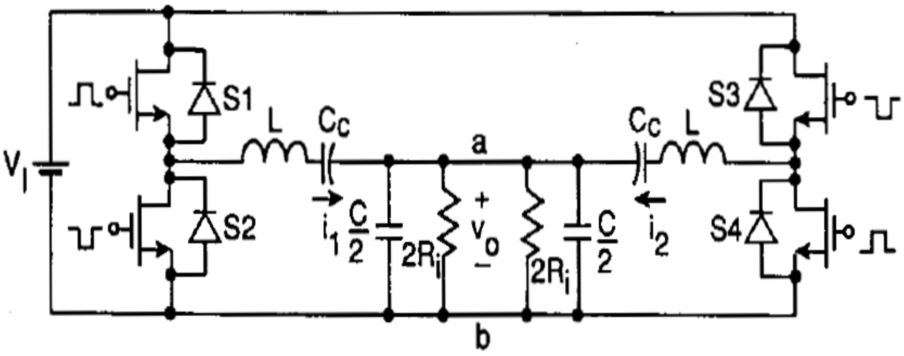

Figure. 3.28: Proposed topology with ac load (M. K. Kazimierczuk, et al., 1993).

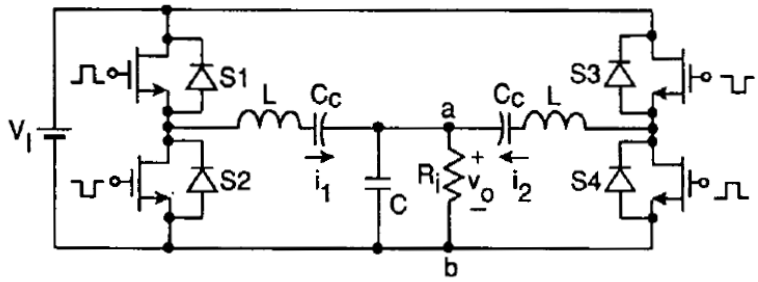

Figure. 3.29: Equivalent circuit with ac load (M. K. Kazimierczuk, et al., 1993)

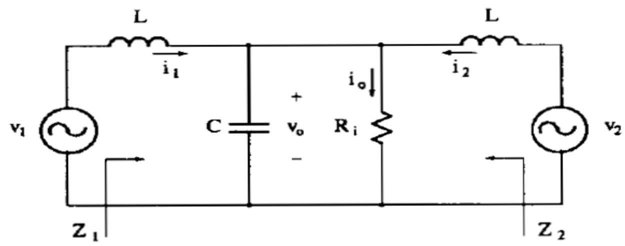

Figure. 3.30: Main equivalent circuit (M. K. Kazimierczuk, et al., 1993)

$$R_i = \frac{V_{Rim}}{I_{Rim}} \tag{3.25}$$

$$M_R = \sqrt{\frac{\eta_R R_L}{R_i}}(\tag{3.26}$$

$$\eta_R = \frac{P_o}{P_o+4P_D+P_L+P_C} \tag{3.27}$$

A single phase dc to ac to dc circuit is presented in (U. Kundu, P. Sensarma, et al.,2015) with a high frequency transformer link between the load and the source. The resonant tank of the presented topology is of LLC type and it's applied in automatic tracking systems. Figure.3.31 shows the structure of the proposed topology and it's composed of three main parts; the H-bridge structure at the input side connected to the resonant tank and transformer and finally to the rectifier circuit. The resonant tank has the following expressions:

The impedance is given by:

$$Z_{i\infty} = \left(sL_s + sL_p\right)\left(\frac{1+\frac{s^2}{\omega_0^2}}{1+\frac{s^2}{\omega_1^2}}\right) \tag{3.28}$$

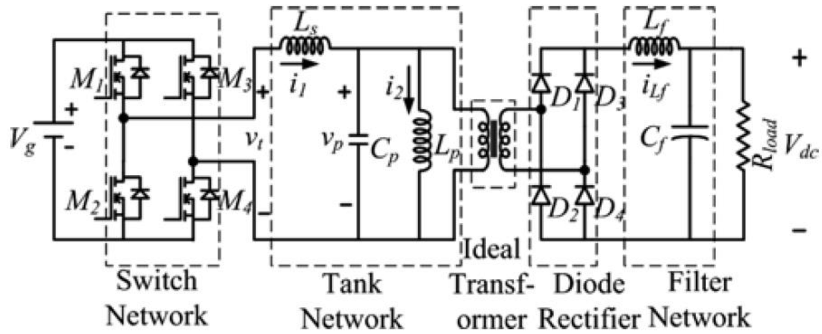

Figure. 3.31: Parallel RC

A new modulation scheme for the control of dc-dc parallel RC is presented in (M. M. Ghahderijani, M. Cactilla, et al., 2017). The proposed control method is the frequency modulation. There are two configuration for the chosen control technique. The first configuration is known as the basic configuration and its made-up three parts:

- External voltage loop
- Internal current loop
- Frequency modulator

These three configurations all have specific functions, the output voltage is controlled by the voltage loop, the input current restriction and the system variations is done by the current loop whiles the frequency modulator protects resonant tank component values against fluctuations. The second configuration which is termed as improved configuration presents a feed forward term which derived as an output component from the inductor current and it's responsible for enhancing the response of transient when there's a rapid variation in the load condition. Figure. 3.32 shows the structure of the presented topology. This converter is a current and classified as a class D converter. Two switches connected in parallel forms the input section, the resonant tank and the HF transformer forms the mid-section and the rectifier plus filter forms the output section.

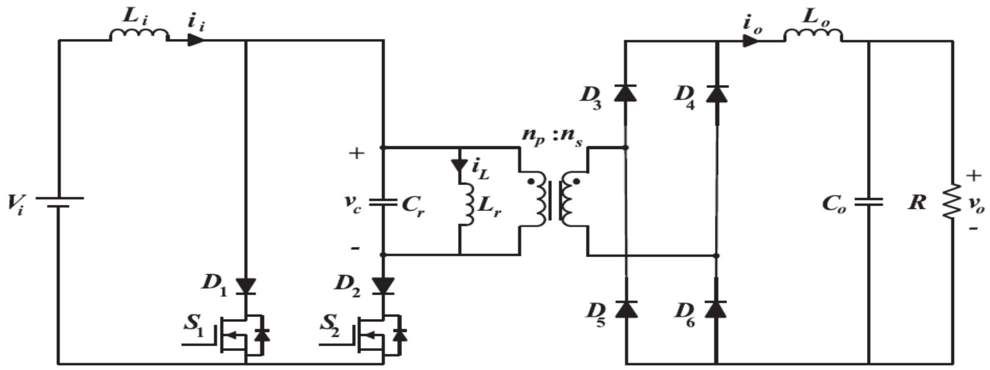

Figure. 3.32: Class D-PLRC

The following expressions are valid for analyzing the converter:

$$I_i = \frac{V_O^2}{V_i R} \tag{3.29}$$

$$V_c = \frac{2V_i}{M} \tag{3.30}$$

$$V_o = \frac{2V_i n_s}{M n_p} \tag{3.31}$$

$$I_O = \frac{1}{R} V_o \tag{3.32}$$

$$M = \frac{1}{\sqrt{1+\left[\frac{Q\pi^2}{8}\left(\frac{n_S}{n_p}\right)\left(\frac{\omega_S}{\omega_p}-\frac{\omega_O}{\omega_S}\right)\right]^2}} \tag{3.33}$$

A new converter is proposed in (M. Kim, H. Jeong, et al., 2018) which is operates with limited switching frequency, this converter tolerates output voltage with wide variations. The switching states of the presented converter allows for ZVS during the turn-on of the semiconductor switches and ZCS during the period of turn-off of semiconductor diodes. Also this converter is suitable for high power applications and at startup, the resonant tank does not experience voltage stress because at notch resonant frequency the voltage gain is zero. Figure. 3.33 shows the structure of the proposed converter which is made up of the usual sections; the H-Bridge structure as the input side, the resonant tank as the mid-section and the H-Bridge rectifier circuit as the output section. The resonant tank of this topology has the following components: two inductors, one capacitor and one transformer. The parallel connection is obtained between the transformer and the notch resonant tank. There are three modes of operation of the converter which are represented by Figure. 3.34. The resonant circuit equivalent circuit are shown by Figure. 3.36. To better understand the modes of operation, let’s refer to Figure. 3.35 which shows the output waveform and the period of switching. The first mode (Figure. 3.34a) correspond to the time period of $t_o - t_1$, the second mode (Figure. 3.34b) of operation correspond to $t_1 - t_2$ and finally the last mode (Figure. 3.3ec) of operation correspond to the time period t_2-t_3. The resonant tank equivalent circuits correspond to the mode of operations and a comparison of the proposed topology to other topologies is shown in Figure. 3.37.

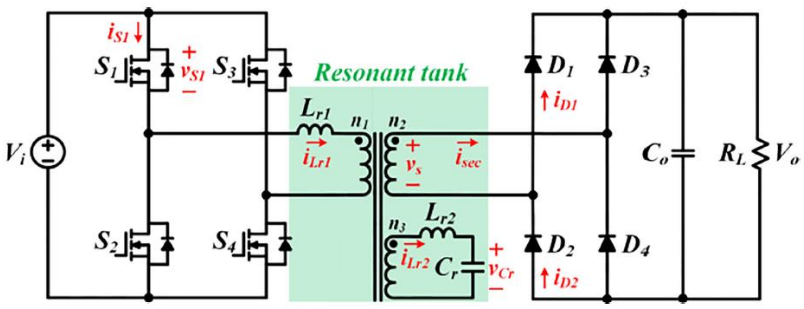

Figure. 3.33: Presented converter

3.4 Series-Parallel-Loaded RC (SL-RC) Topologies

The series-parallel loaded resonant converter is a combination of the series and the parallel RC structures. Depending on the converter topology, SPL resonant converter is connected at the output of the converter to provide high efficiency by reducing the switching losses of the converter when zero-voltage and zero-current switching is attained. Some selected papers on the above mentioned subject are presented below.

Analysis and implementation of a novel series-parallel resonant converter is presented in (M. A. Halim, et al., 2013), the resonant tan is of LLC nature and it's embedded in a half H-Bridge topology. Figure. 3.38 shows the structure of the proposed converter. The equivalent circuit of the proposed topology is shown by Figure. 3.39.

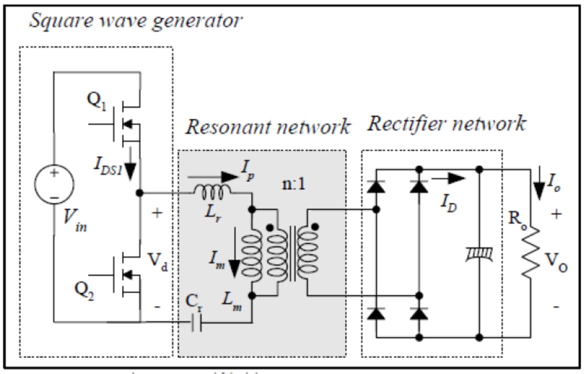

Figure. 3.38: Series-Parallel RC

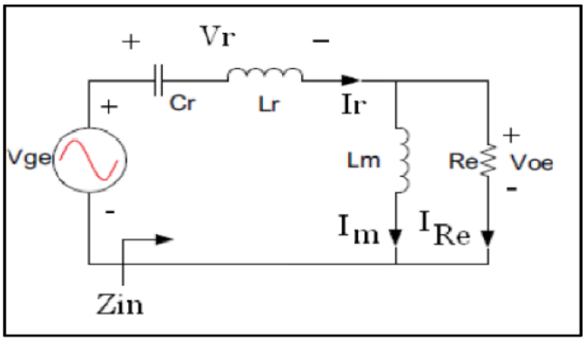

Figure. 3.39: Equivalent circuit

The voltage gain is given by:

$$V = 2n\frac{V_o}{V_{in}} \tag{3.34}$$

An LCL based series-parallel RC is presented in (W. Wu, Y. Sun, et al., 2014). Analysis of this converter with respect to the harmonic content and interferences caused EMI is investigated. Most importantly the ability to reduce the harmonic current located in the surroundings of the switching frequency will lead to reduction in the size of induction hence the volume and size of the converter will be reduced and the converter cost will also be reduced. The structure of the presented topology is given by Figure. 3.40, the resonant tank is composed of two tanks and it’s a modified system which is a better harmonic injection network when compared to the conventional structure. The transfer function relationship is given by:

$$G = \frac{1/sC_f}{(sL_1+R_1)Z_2+(sL_1+R_1)\left(\frac{1}{sC_f}\right)+Z_2(sC_f)} \tag{3.35}$$

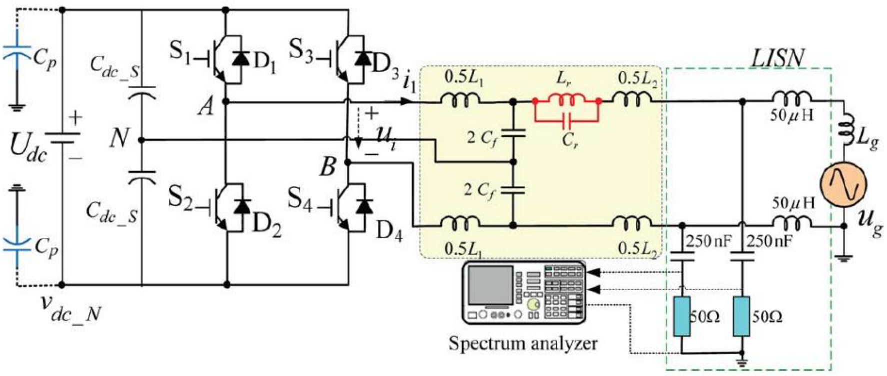

Figure. 3.40: LCL converter

In (N. Shafiei, W. Eberle, et al., 2014), investigation of the effects of pure capacitor filter at the output of resonant tank based converters is carried out. The resonant tank is a combination of PLRC and the series-parallel LRC. The conventional resonant tank based rectifiers have problems with power transfer between the primary and secondary sections. Hence employing the formal formulas to analyze the component behaviors is not acceptable. A new method of analyses is done with this new topology with respect to the design analysis.

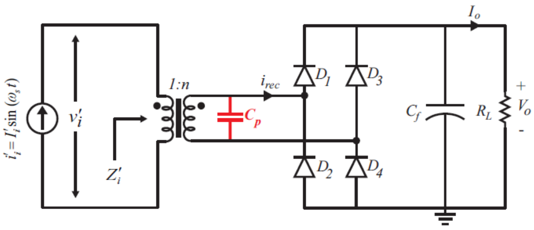

Figure. 3.41: Capacitor output filter

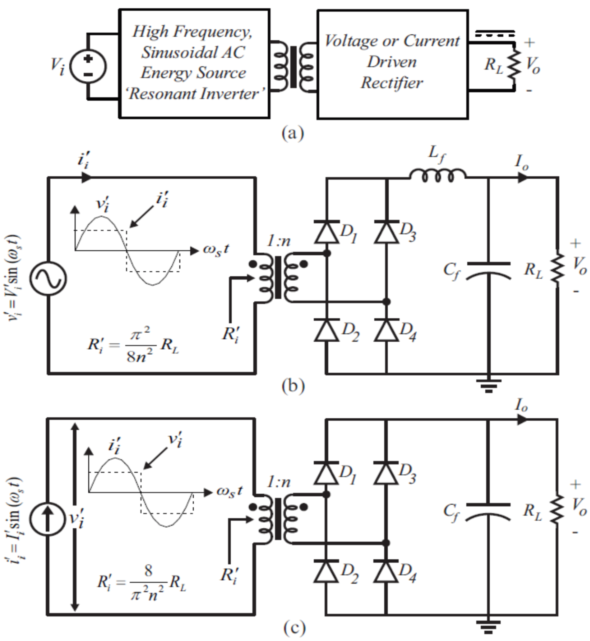

Figure. 3.42: Various resonant tank structures

Figure. 3.42 shows the resonant tank with various converter structures, in Figure. 3.42a shows the main resonant tank, Figure. 3.42b shows topology with a voltage source and Figure. 3.42c shows the topology with a current source. Detailed analyses with the appropriate equations have been provided in (N. Shafiei, W. Eberle, et al., 2014)

In (R. Yang, H. Ding, et al., 2014), investigation of the effects of pure capacitor filter at the output of resonant tank based converters is carried out. The resonant tank is composed of LCC structure. A new function called piecewise analytic is proposed to investigate the steady state features of the proposed converter. The converter is operated in the DCM mode and has two equivalent circuit of sequence. Figure. 3.43 shows the structure of the presented converter which is composed the two H-Bridges, one been an inverter and the other being a rectifier. The resonant tank coupled with the transformer is sandwiched between the two structures. The output filter is compose of only a pure capacitor connected in parallel with the load. There are seven modes of operation which shown by Figure. 3.44.

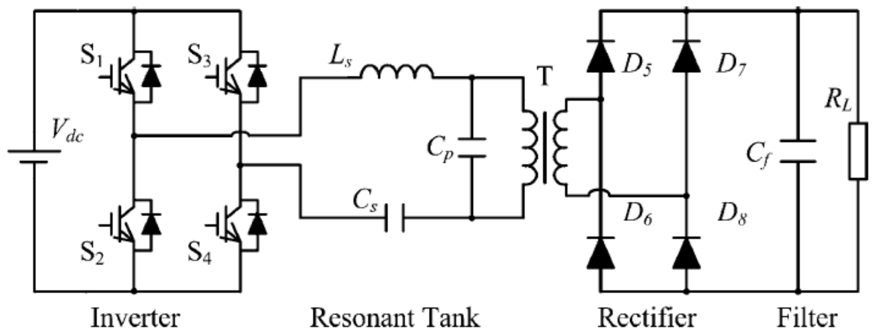

Figure. 3.43: LCC tank based converter (N. Shafiei, W. Eberle, et al., 2014)

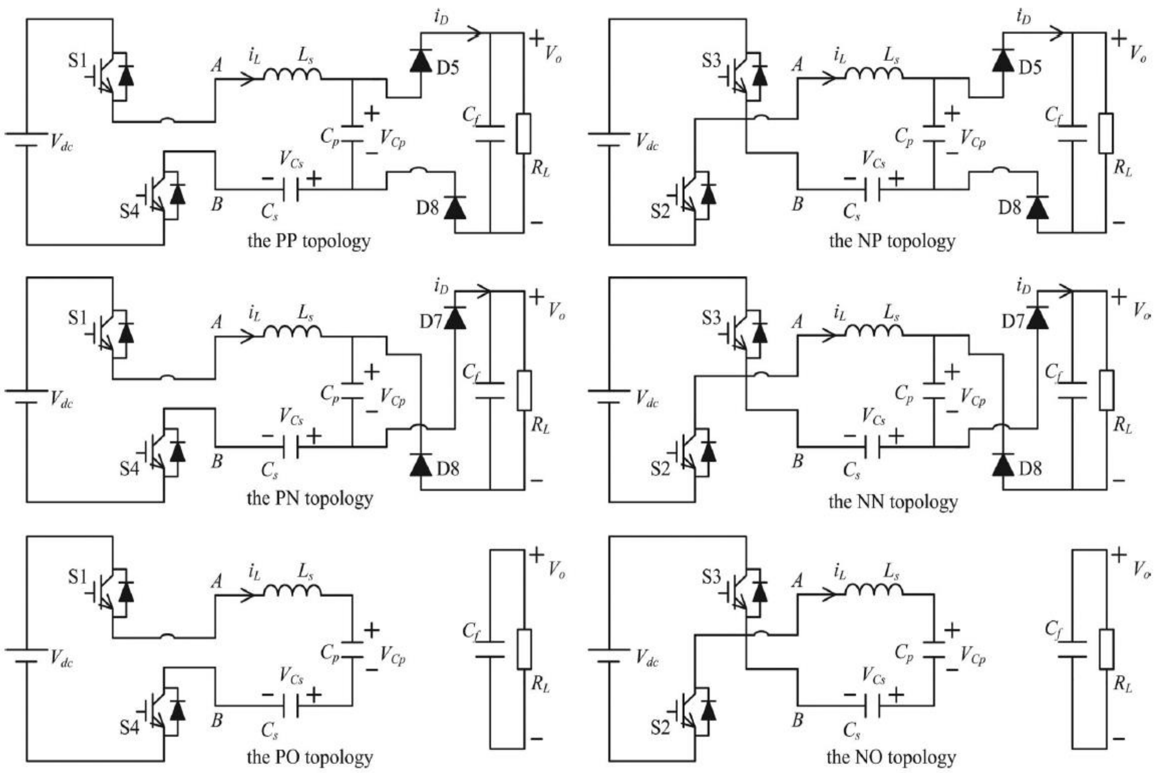

Figure. 3.44: Modes of operation(N. Shafiei, W. Eberle, et al., 2014)

Some useful expressions of the proposed topology are:

Resonant impedance is expressed as:

$$Z_r = \sqrt{\frac{C_p + L_s C_s}{C_s C_p}} \tag{3.36}$$

Resonant frequency (angular) is expressed as:

$$\omega_r = \sqrt{\frac{C_s + C_p}{C_p L_s C_s}} \tag{3.37}$$

The voltage gain is expressed as:

$$G = \frac{2\lambda}{n_c + 1} \tag{3.38}$$

The power factor is expressed as:

$$Pf = \frac{\int_0^{T_{iL}} i_L(t)dt}{\sqrt{\int_0^{T_{iL}} i_L^2(t)dt}\sqrt{T_{iL}}} \tag{3.39}$$

An interleaved resonant tank based converter is analyzed with respect to the load sharing attributes (G. Yang, P. Dubus, et al., 2012). The series-parallel RC with LLC structure constitutes the resonant tank. The connection of the resonant tank to the converter is that the primary side is connected in series and the secondary side is connected in parallel. Fundamental approximation method is used to derive the equivalent circuit for analysis. Figure. 3.45 shows the presented converter with a single cell LLC RT. The equivalent circuit is represented by Figure. 3.46.

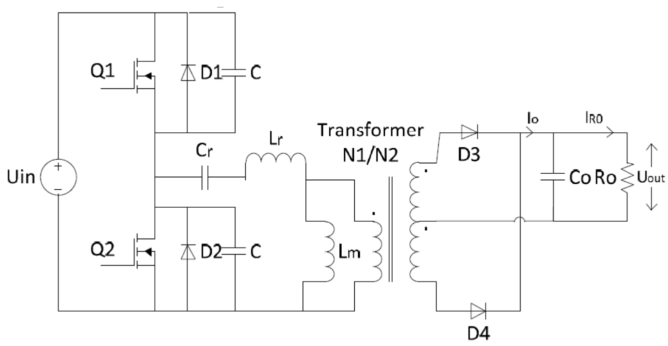

Figure. 3.45: Presented topology in (G. Yang, P. Dubus, et al., 2012).

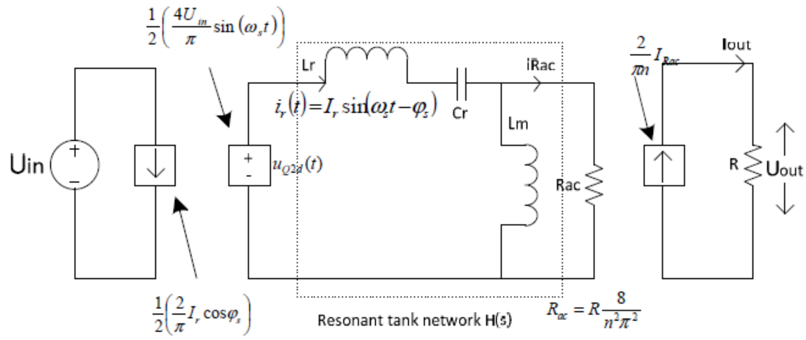

Figure. 3.46: Equivalent circuit(G. Yang, P. Dubus, et al., 2012).

The input current is expressed as:

$$i_{in} = I_r cos\varphi_s \frac{1}{\pi} \tag{3.40}$$

The gain is expressed as:

$$G = \frac{1}{\left(1+\lambda-\lambda\frac{1}{f_n^2}\right)+jQ\left(f_n-\frac{1}{f_n}\right)} \tag{3.41}$$

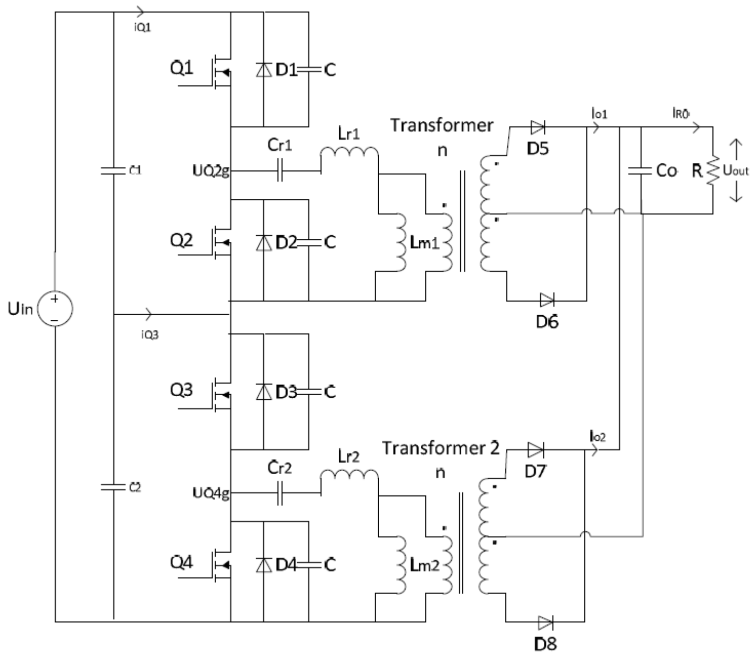

Figure. 3.47: Proposed interleaved SPRC (G. Yang, P. Dubus, et al., 2012)

3.5 Hybrid RC (H-RC) Topologies

A hybrid resonant converter controlled by PWM technique is presented in (W. Yu, j. S. Lai,et al., 2012). The half H-Bridge converter provides soft switching and is controlled by phase shift PWM. The overall converter is a combination of half and full H-Bridge structures. The presented control technique ensures that the soft switching of ZV is achieved for the leading leg for variations of load conditions from minimum to maximum load whiles the lagging leg also experiences the switching states of ZC where minimum leakage inductance leads minimum conduction loss and minimum duty cycle losses. The structure of conventional resonant tank based converter is represented by Figure. 3.48a to Figure. 3.48c. The topology of Figure. 3.48a is capable of zero voltage switching and the only one transformer acts as the link between the structures, however the structure of Figure. 3.48b is capable of switching at both zero voltage and zero current and also with only one transformer and finally the structure of Figure. 3.48c is similar to the structure of Figure. 3.48a but has two transformers. Figure. 3.49 shows the structure of the presented topology which is composed of two parts; the half bridge with the resonant tank and the full bridge controlled by phase shift PWM. The presented topology combines two converter techniques which are that of LLC and the phase shifted PWM.

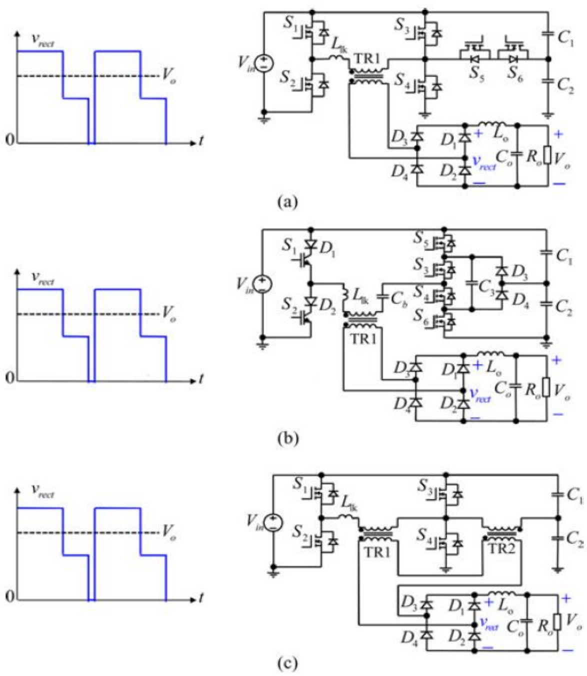

Figure. 3.48: Full and half HB converters (W. Yu. J. S. Lai, et al., 2012).

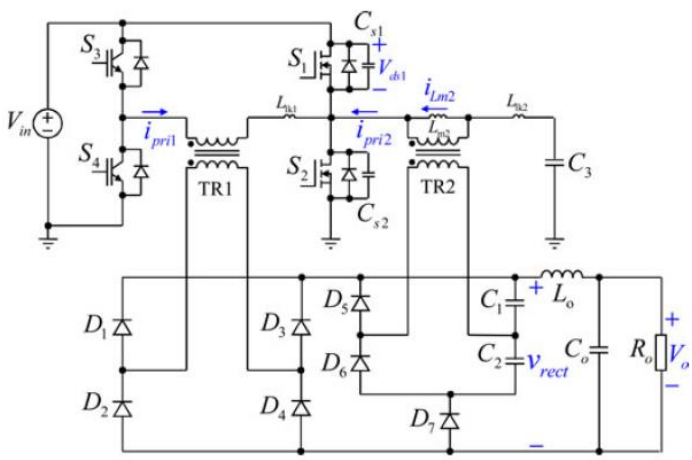

Figure. 3.49: Presented converter(W. Yu. J. S. Lai, et al., 2012).

A flying capacitor based resonant converter is presented in (W. Li, Q. Luo, et al., 2016). This converter is applied in step-down of voltage in high power systems. The major advantage of the flying capacitor topology when compared to the half H-bridge is its ability to reduce the stress voltage to half. And also equal sharing of the source voltage across the switches without employing extra control circuit or balancing circuit is another advantage of the flying capacitor topology. Also the soft switching provided by the resonant tank will minimize the switching losses and improve the efficiency of the converter. The following Figures shows the various topologies of flying capacitor and half HB based resonant tank converters which aids the authors to develop the presented topology.

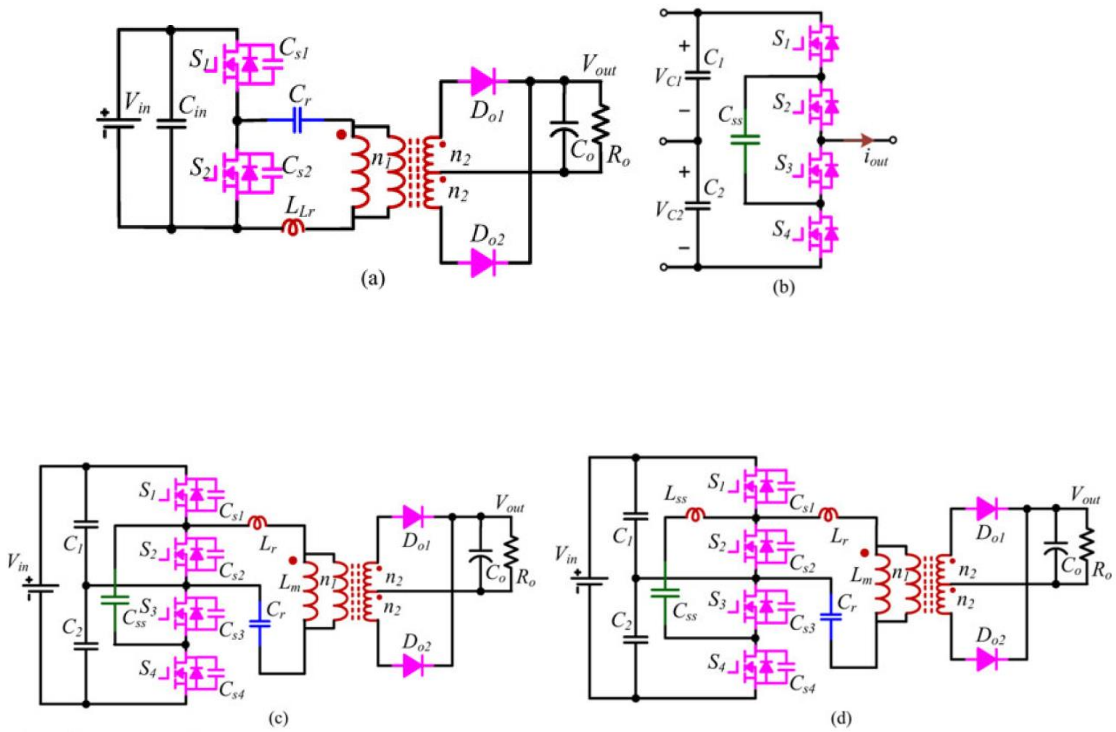

Figure. 3.50: a) Half HB converter

b) Flying capacitor converter

c) Presented FC resonant converter

d) Optimized FC resonant tank converter

The presented converter is shown by Figure. 3.50 and it consist of series connection of two half H-Bridges coupled with a flying capacitor topology to provide the equal sharing of the source voltage by the source capacitors. An LLC resonant tank and a transformer links the output rectifier circuit to the source voltage. There are six stages of operation of the presented converter.

The impedance of the flying capacitor is given by:

$$Z_{FC} = R_S + \frac{1-\left(\frac{1}{\sqrt{L_r C_r}}\right) L_{SS} C_{SS}}{j\left(\frac{1}{\sqrt{L_r C_r}}\right) C_{SS}} \tag{3.42}$$

The voltage gain is given by:

$$M = \frac{1}{\sqrt{\left(1+\lambda-\frac{\lambda}{f_n^2}\right)^2 + \left(f_n - \frac{1}{f_n}\right)^2 Q^2}} \tag{3.43}$$

A novel hybrid converter is presented in (J. H. Kim, et al., 2017). This converter has several advantages over the conventional H-Bridge controlled by PS-PWM. Some of which are: increased ZV switching range, minimum conduction losses and reduced output filter size. The presented converter consist of three parts: full H-Bridge structure, the resonant and the half H-Bridge which is shown by Figure. 3. 51.

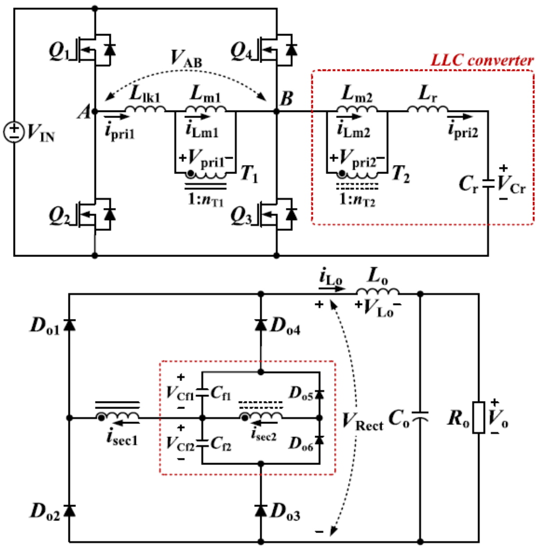

Figure. 3.51: Hybrid LLC converter (J. H. Kim, et al., 2017).

A half H-Bridge hybrid resonant converter for PF correction is presented in (M. Alam, W. Eberle, et al., 2017). This boost converter is suitable for used in battery charging systems and power supply systems. The size of the resonant tank components are small when compared to other topologies. Figure. 3.52 shows the structure of the presented topology which can be described as a bridgeless system hence does not require a separate rectifier circuit. The two can be gated with the same PWM signal therefore separate sensing system for different polarities are required. There are two modes of operation of the converter: the first mode is when the converter switches are on which the hybrid resonant state is and when the converter switches are off, the state is the PWM. Figure. 3.53 shows the current waveforms during the hybrid resonant state.

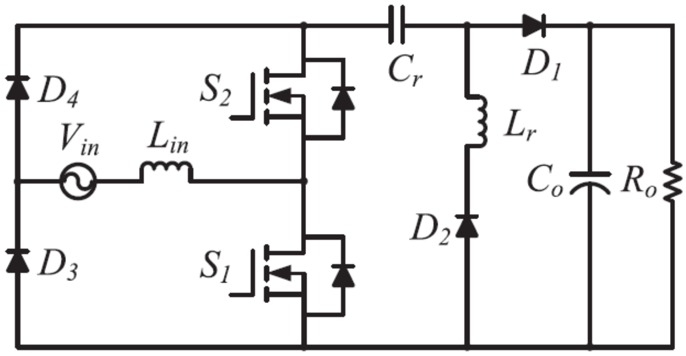

Figure. 3.52: Hybrid resonant converter (M. Alam, W.Eberle, et al., 2017).

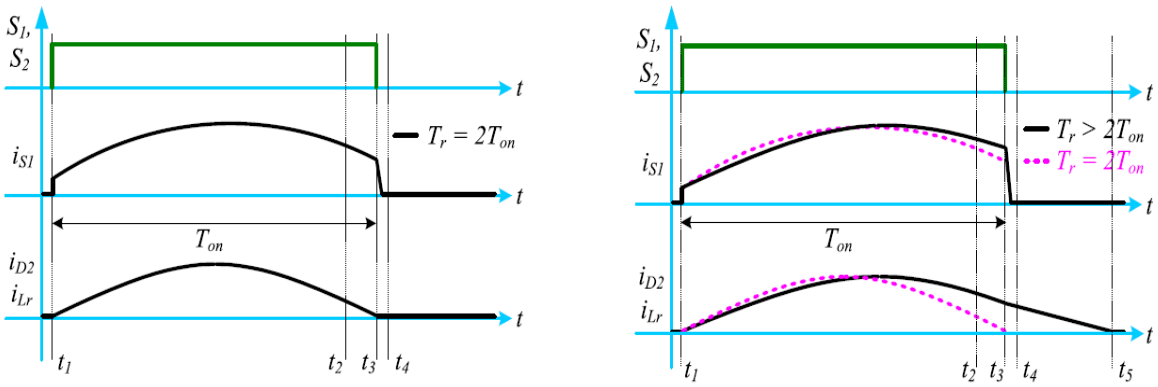

Figure. 3.53: Gating signal waveforms (M. Alam, W.Eberle, et al., 2017).

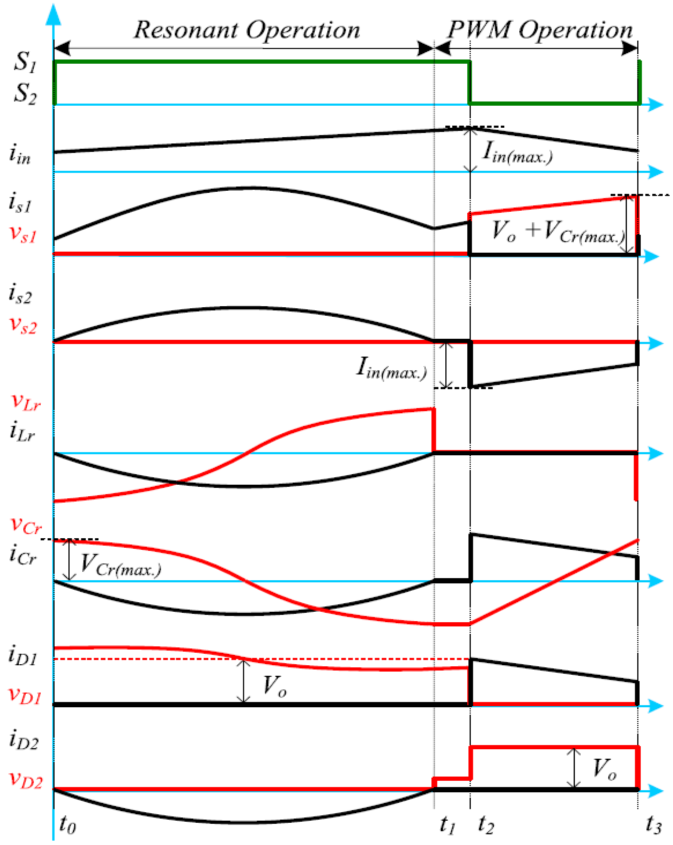

Figure. 3.54: Main output waveforms(M. Alam, W.Eberle, et al., 2017).

The boost factor is given by:

$$B = \frac{1}{1-D} \tag{3.44}$$

3.6 Conclusion

Literature review of resonant converter is investigated in this part of the thesis. Resonant converters (RC) provides the means by which high frequency switching of power electronic converter are possible without any major limitations. Applying resonant switching in high frequency based inverter or power conversion topologies provides the following advantages: minimum inverter size, minimum weight and reduced power loss. The classification of resonant converters is also investigated, however much emphasis is placed on the various types of loaded resonant converters because the proposed topology falls within this group.

CHAPTER 4

PROPOUNDED TOPOLOGY AND SIMULATION RESULTS

4.0 Proposed Topology

Power electronic converters have become principal devices in providing of cheap, efficient, reliable and quality power to the consumer. Basically converters are useful devices in the chain of power supply, they are mostly suitable for power conditioning or providing power with the desired qualities as desired by the consumer or the load.

Induction heating systems have several applications of which induction cooking is one. The advancement in induction cooking technologies have made it such that multiple burners are applicable, these offer better energy and device utilization when compared to the single burner system. The multiple burner systems are made possible by using two or four inductors. In the traditional single burner system, one converter is applied to one burner or one converter is applied to multiple burners.

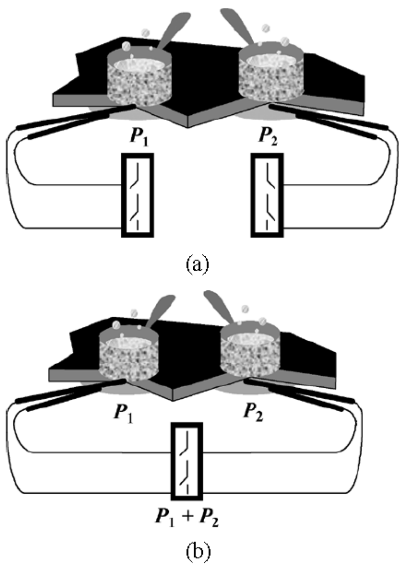

Figure. 4.1: Converter-burner applications

The proposed topology in this research is a novel two output converter which employs series loaded RC in its structure. The structure of the propounded topology is derived from the conventional H-Bridge with the inclusion of two power switches, two outputs with individual series loaded resonant tanks. Basically the propounded topology seeks to combine two H-Bridge series loaded RC into a single converter having two output resonant loads. The structure of the conventional single output converter is indicated by Figure. 4.2whiles the proposed topology is given by Figure. 4.3. The equivalent circuit is given by Figure. 4.4.

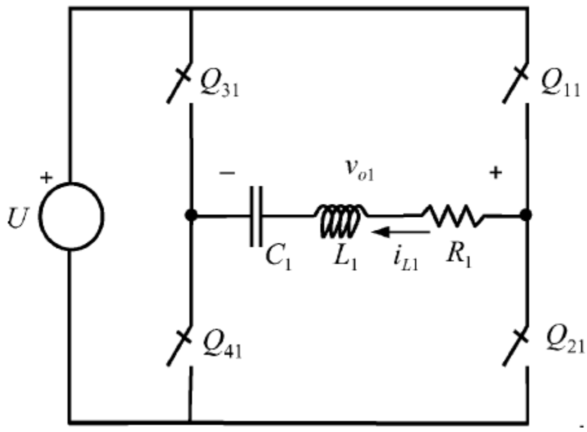

Figure. 4.2: Conventional single output inverter

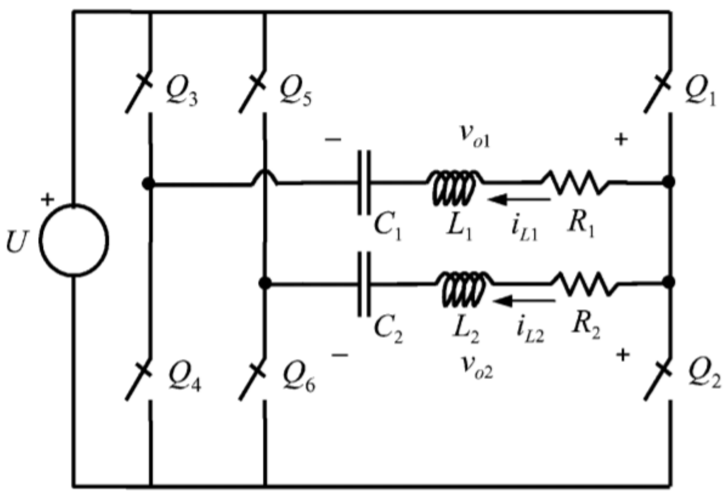

Figure. 4.3: Proposed two output converter

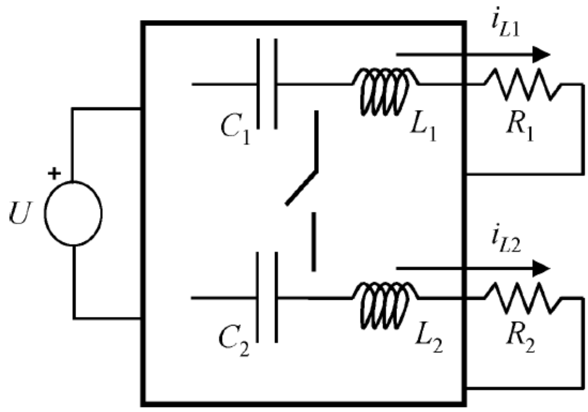

Figure. 4.4: Equivalent circuit

The possible output waveforms for the two outputs using the asymmetric voltage control technique is shown by Figure. 4.5. The generalized control method of AVC is shown by Figure. 4.5a and the superlative method of AVC is given by Figure. 4.5b.

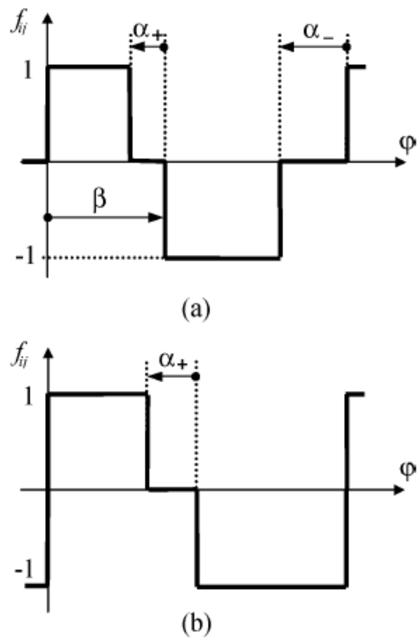

Figure. 4.5: AVC control method

The mathematical expressions governing the proposed method are given below:

The energy state equation is given below:

$$\begin{bmatrix} L & 0 \\ 0 & C \end{bmatrix} \begin{bmatrix} i'_L \\ v'_C \end{bmatrix} = \begin{bmatrix} -R & 1 \\ -1 & 0 \end{bmatrix} \begin{bmatrix} i_L \\ v_C \end{bmatrix} + \begin{bmatrix} f_j \\ 0 \end{bmatrix} U \tag{4.1}$$

The two state variables are:

$$i_L = \begin{bmatrix} i_{L1} \\ i_{L2} \end{bmatrix} \tag{4.2}$$

$$v_C = \begin{bmatrix} v_{C1} \\ v_{C2} \end{bmatrix} \tag{4.3}$$

The identity matrix for the resonant components are:

$$R = \begin{bmatrix} R_1 & 0 \\ 0 & R_2 \end{bmatrix} \tag{4.4}$$

$$L = \begin{bmatrix} L_1 & 0 \\ 0 & L_1 \end{bmatrix} \tag{4.5}$$

$$C = \begin{bmatrix} C_1 & 0 \\ 0 & C_2 \end{bmatrix} \tag{4.6}$$

$$-Ri_L + f_J U + v_C = L\frac{di_L}{dt} \tag{4.7}$$

$$-i_L = C\frac{dv_C}{dt} \tag{4.8}$$

The magnitude of the output voltage or peak to peak value is given:

$$\frac{1}{2}\left(Ri_L + L\frac{di_L}{dt} - v_C\right) = f_j \tag{4.9}$$

The desired control of the proposed two output together with converter structure is shown by Figure. 4.6. The converter structures are the same however the control techniques are not, the upper waveform of Figure. 4.6 is the conventional AVC control technique and the lower

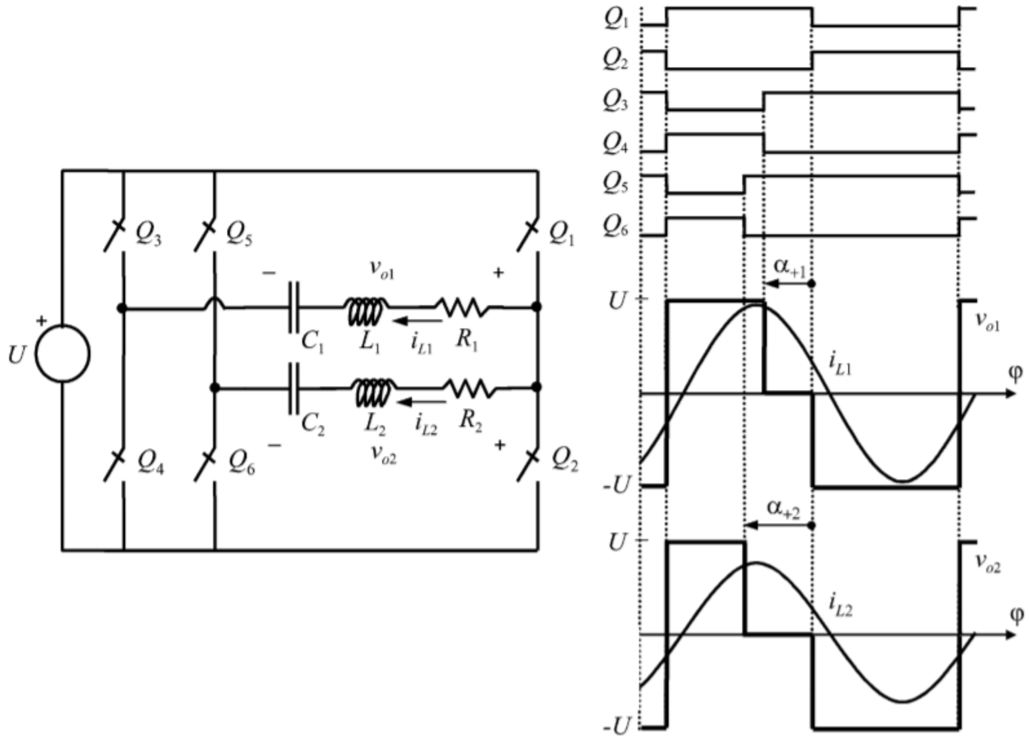

Figure. 4.6: Proposed converter and output waveforms

The modes of operating the proposed two output inverter is analyzed according to the two load waveforms as shown in Fig. 4.6; the various segments of the desired waveform determines the operating states of the proposed topology. Table 4.1 shows the states or modes of operating which will generate the desired load waveform for the first output and second output. There are five states of operations for the two outputs as shown by Table 4.1.

Table 4.1: Switching States of First Output

State	On switches	Off switches
I	Q_2, Q_3, Q_5	Q_1, Q_4, Q_6
II	Q_1, Q_4, Q_6	Q_2, Q_3, Q_5
III	Q_1, Q_4, Q_5	Q_2, Q_3, Q_6
IV	Q_1, Q_3, Q_5	Q_2, Q_4, Q_6
V	Q_2, Q_3, Q_5	Q_1, Q_4, Q_6

4.1 Converter Loss

Determination of the converter losses are carried out in this section of the thesis. The losses of a converter is made up of switching losses and conduction losses and at times blocking voltage power losses. However switching losses and conduction losses only will be analyzed in this section. Switching losses occur during the states of switching or changing the states of the power switches whiles conduction losses occur during the period in which the switches are gated on.

4.2 Switching Losses

The switching losses of the proposed converter is determined by the equation below. Let P_{SW} ,represent switching power loss, P_{on} represent the turn-on power loss and P_{off} represent the turn-off power loss.

$$P_{SW} = P_1 + P_0 \tag{4.10}$$

$$P_{on} = \frac{1}{T_S}\int_0^{t_{on}} v_s i_s dt \tag{4.11}$$

$$P_{off} = \frac{1}{T_S}\int_0^{off} v_i i_s dt \tag{4.12}$$

4.3 Conduction Losses

Conduction loss of a semiconductor switch occurs during the operational period of the switch and blocking loss occurs during the non-conduction period or the open state of the switch. Both power losses are represented by:

$$P_{conduction,av} = \frac{1}{T_s}\int_0^{T_{on}} v_s i_s dt \tag{4.13}$$

$$P_{conduction,av} = \frac{1}{T_s}\int_0^{T_{on}} V_{on} I_{on} dt \tag{4.14}$$

The total converter power loss is given by:

$$P_{Total\ loss} = P_{SW} + P_{conduction} \tag{4.15}$$

Therefore efficiency of the converter is given by:

$$Efficiency = \frac{P_{in} - P_{Total\ loss}}{P_{in}} \tag{4.16}$$

Where P_{in} is the input power of the inverter and P_{out} is the output power of the inverter.

4.4 Simulation Results

Simulation implementation of the proposed two output converter is carried out in MATLAB R2015a software edition. All switches used are IGBT connected with antiparallel diodes to constitute bidirectional flow path for current and unidirectional flow path for voltage. In other to reduce switching losses especially during the period of turn-off, snubber capacitor with magnitude of 10nanoF is connected to all IBGTs. Table 4.2 shows the parameters used for simulation. Modeling of the proposed converter in Matlab Simulink is into three main parts which shown by Figure. 4.7 toFigure. 4.8. The first is the control signal generations, the second is the control of the H-Bridge structure and finally the third part is the control of the whole converter structure.

Table 4.2: Parameters for Simulation

Component	**Value**
Input Voltage V_{in}	325V
Switching frequency f_{sw}	48kHz
Output inductor L_o	60 µH
Output capacitor C_o	450Nf
Output resistor R_o	9.5Ω

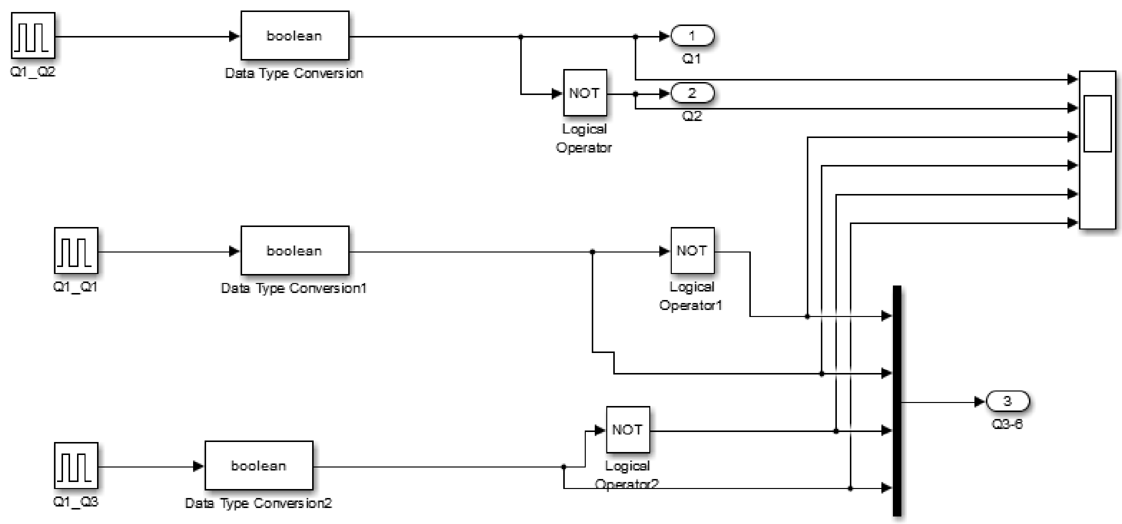

Figure. 4.7: Gate signal generation

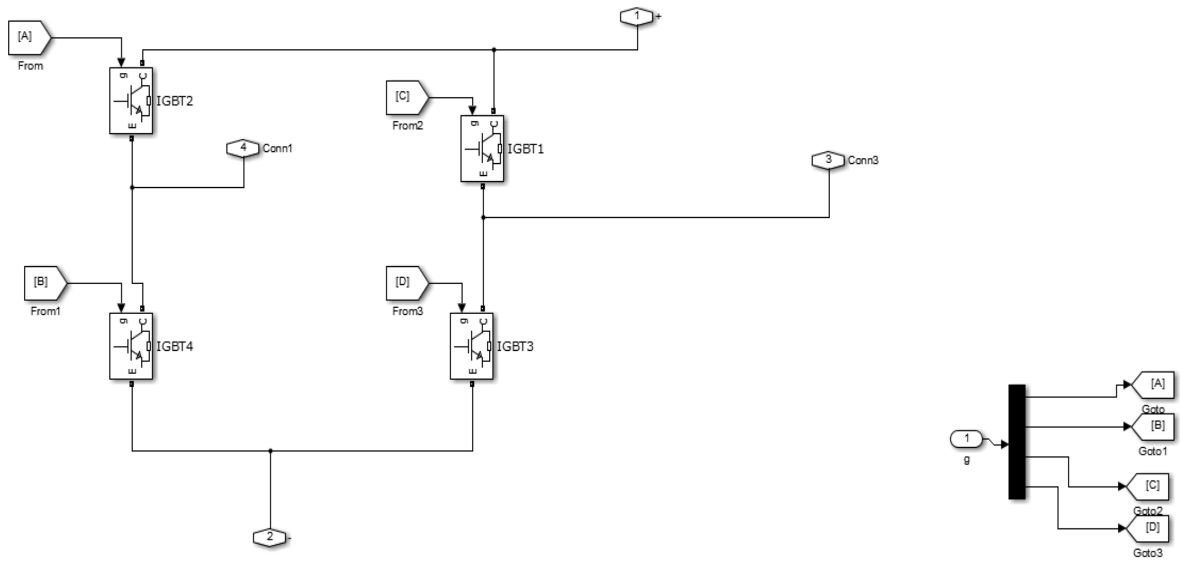

Figure. 4.8: HB structure control

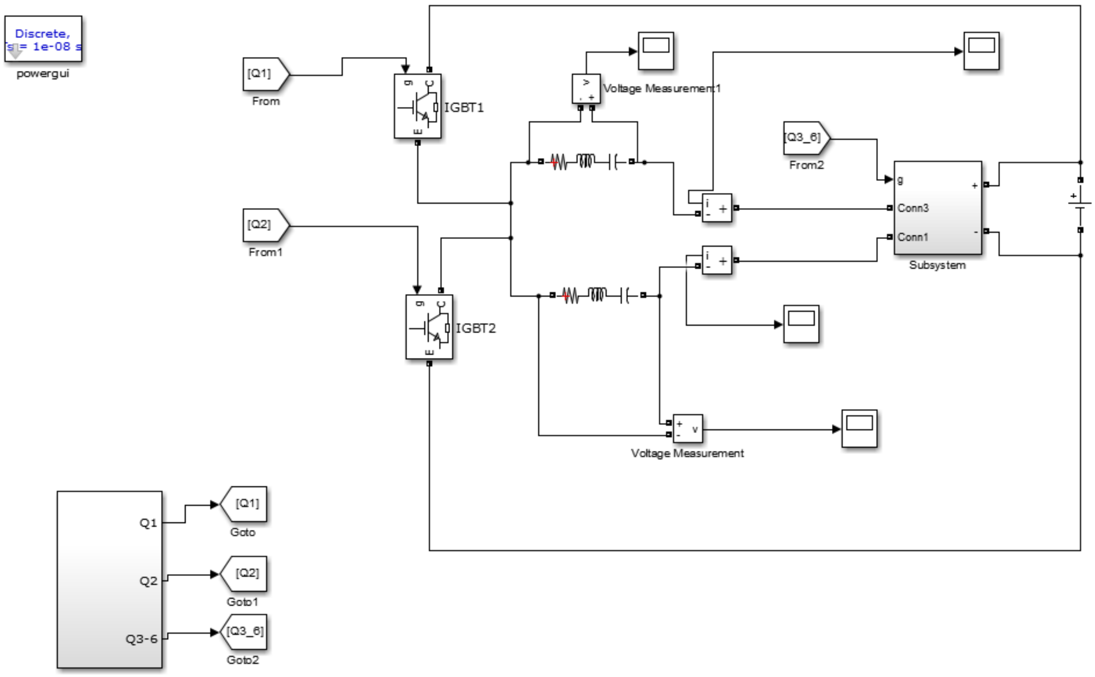

Figure. 4.9: Proposed converter control

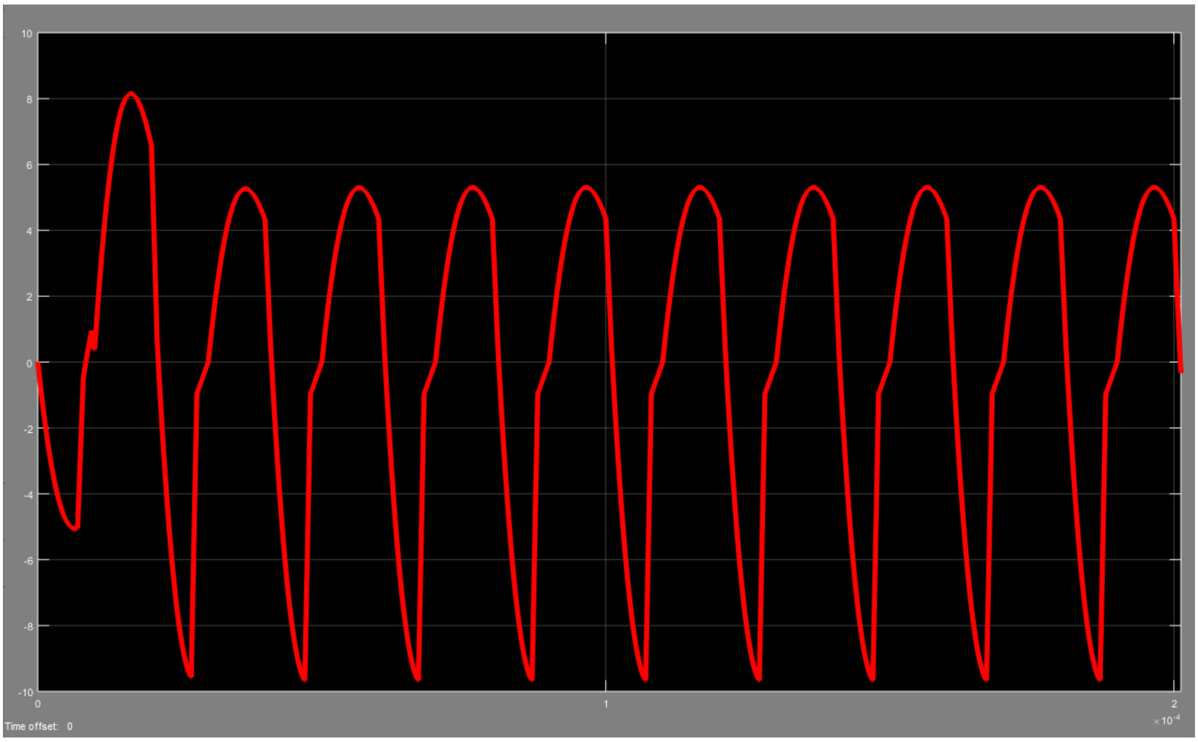

Figure. 4.10: Output one inductor current waveform

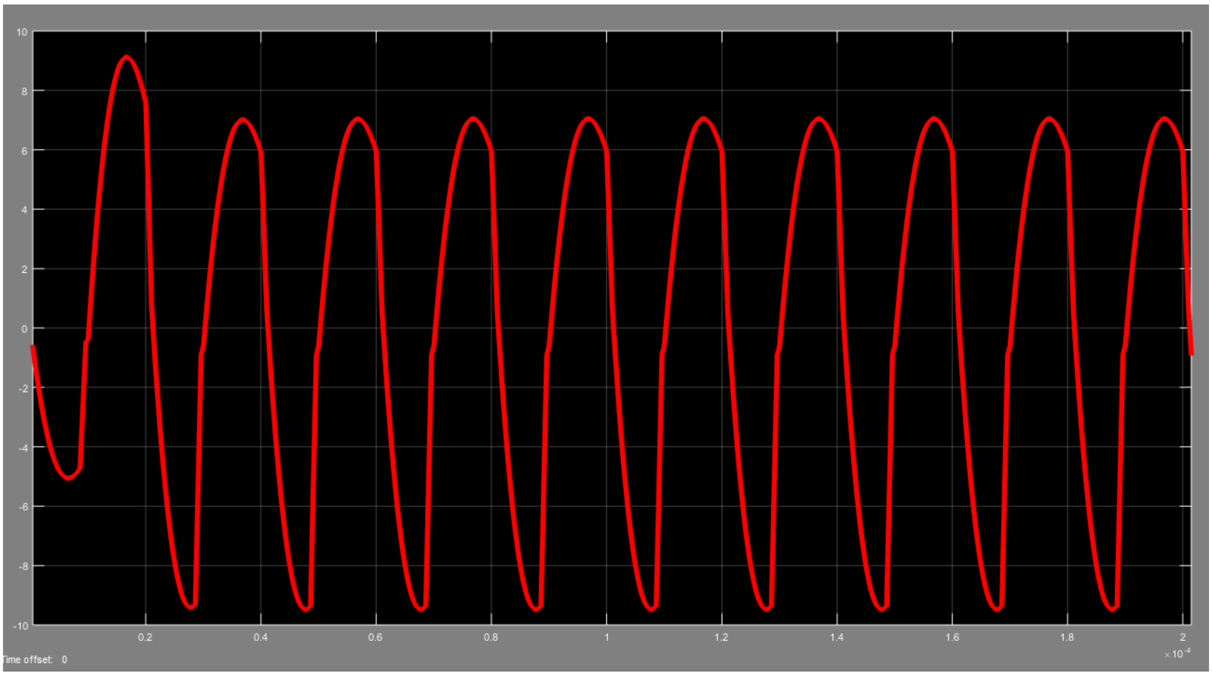

Figure. 4.11: Output two inductor current waveform

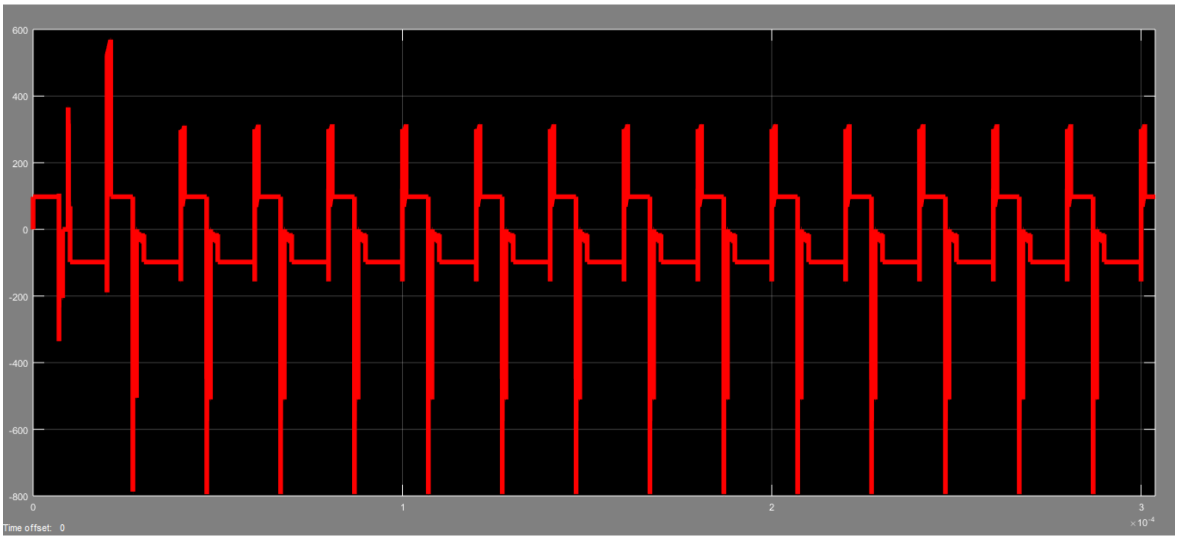

Figure. 4.12: Output one voltage waveform

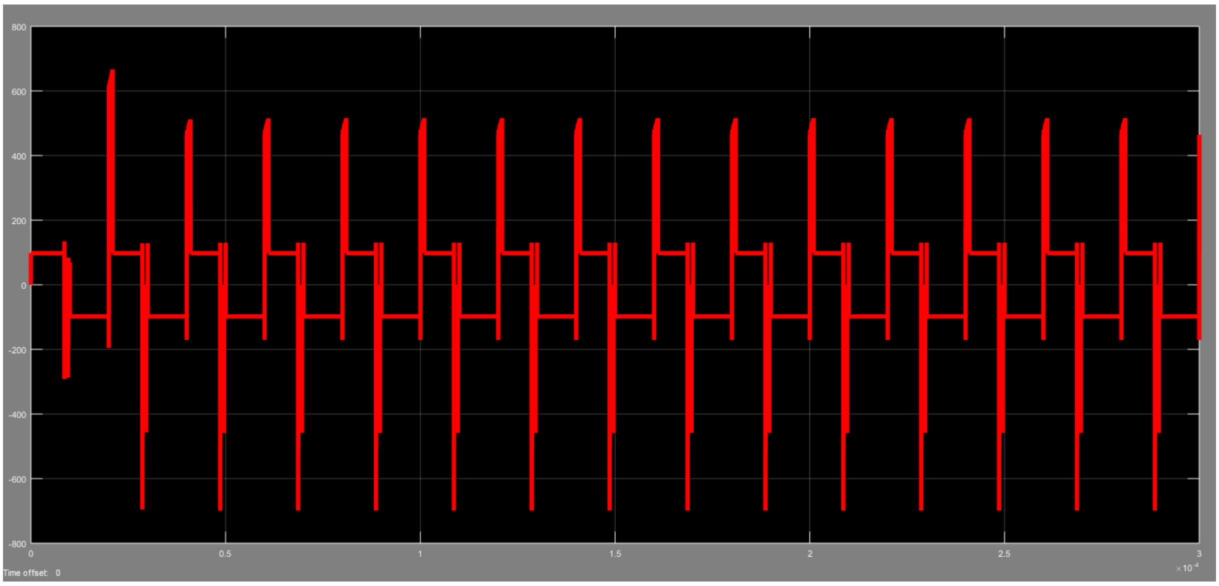

Figure. 4.13: Output two voltage waveform

The proposed two output series RC was successfully implemented in MATLAB R2015a environs using the parameters indicated in Table 4.1. The load of the two output systems uses the same values for the RLC. Two waveforms are generated from the simulation; these are the voltage and current waveforms. Figure 10 and Figure 4.11 shows the inductor current waveform for the first output and second output respectively. Similarly, the generated voltage waveforms across the RLC load for the first output and second output are illustrated by Figure 4.12 and Figure 4.13 respectively. For experimental investigations, a mechanical switch will be placed across the two output to enable alternating applications of the outputs.

4.5. Conclusion

The simulation of the proposed two output inverter coupled with a series resonant tank is presented in this section. The proposed topology is an enhancement of the conventional HB structure which is composed of only one output. The proposed topology is derived by adding two unidirectional switches to the HB topology therefore being able to provide two output simultaneously. The load voltage and current waveforms derived from simulation using the parameters of Table 4.1 authenticates the theoretical analysis provided in this section.

CHAPTER 5

CONLUSION AND RECOMMENDATIONS

5.0 Conclusion

The goal of this research is to investigate the application of two output inverter systems for induction cooking applications. The proposed converter seeks to eliminate the need for multiple inverters for multiple burner applications by developing a new converter topology which has two output systems hence can be applied in multiple burner applications. The proposed topology is derived by adding two unidirectional switches to the conventional structure as shown in the simulation circuit. Application of snubber capacitors in the transistor switches minimizes the switching losses and also the application of series resonant tank provides safe commutation and reduces losses due to switching. Hence the propounded converter can boast of increased efficiency when the switching losses are minimized. There's a direct correlation between the losses produced by the converter and its efficiency. When the overall converter losses are minimized, the converter efficiency is maximised and when the converter losses are increased, the efficiency is reduced. Finally the proposed converter topology is achieved by utilizing minimum component count when compared to two single output inverter systems. The reduced component count also increases the efficiency, reduce the size and weight of the converter and finally the converter cost is also minimised.

5.1 Recommendations

As part of future works or recommendation, I wish to implement the proposed converter by experimentation to investigate its actual working principles in the laboratory. Finally I would also like to investigate if the output systems can be increased from two to four and analysis the necessary topology which will boast or maximise the voltage gain capabilities of the proposed topology.

REFERENCES

A. Lesnicar, R. C. Marquadt. (2004). A new modular voltage source inverter topology. *Institute of Power Electronics and Control, Universität Bundeswehr München, Werner-Heisenberg-Weg, 12*(2), 124-131.

A. Masaoud, H.W. Ping, S. (2014). New three-phase multilevel inverter with reduced number of power electronic component. *IEEE Trans. Power Electron., 29*(11), 6018-6029.

A. Nabae, I. Takahashi and H. Akagi, (1981). A new neutral-point clamped PWM inverter. *IEEE Trans, 17*(5), 518-523.

A.L. Batschauer, S.A. Mussa, and M.L. Heldwein. (2007). Three-phase hybrid multilevel inverter based on half-bridge modules. *IEEE Trans. Ind. Electron., 59*(2), 668-678.

AbdAlmula Gebreel. (2012). Survey on Topologies, and Control Techniques for the Most commom Multilevel Inverters. *In International Journal of Scientific & Engineering Research,* (vol. 6,6, pp. 2229-2250).

Alian Chen, Xiangning He. (2006). Research on Hybrid-Clamped Multilevel-Inverter Topologies. *IEEE Transactions on Industrial Electronics, 53*(6), 1898-1907.

B.-S. Suh, D.-S. Hyun. (1997). A new N-level high voltage inversion system. *IEEE Trans. Ind. Electron., 44*(1), 107–115.

C. C. Lee, L. L. Hon. (2017). Critical Study on the Relationship between Power Conversion Technique and Energy Efficiency on Induction Cooker. *In IEEE International Symposium on Product Safety and Compliance Engineering - Taiwan (ISPCE-TW)*(vol. 45,3, pp. 1-2).

E. Babaei, S. H. Hosseini, (2009). New cascaded multilevel inverter topology with minimum number of switches. *Energy Conversion and Management*, *50*(5), 2761-2767.

E. Babaei, S. Laali. (2016). New extendable 15-level basic unit for multilevel inverters. *Circuits Syst. Computer, 25*(1–22), 165-151

E. Babaei. 2017. A cascade multilevel converter topology with reduced number of switches. *IEEE Trans. Power Electron.*, 23(6), 2657-2664.

E. Babaei, M. FarhadiKangarlu, and F. NajatyMazgar. (2008). Symmetric and asymmetric multilevel inverter topologies with reduced switching devices. *Elect. Power Syst. Res., 86*(2), 122-130.

E. Babaei, M.S. Moeinian. (2010). Asymmetric cascaded multilevel inverter with charge balance control of a low resolution symmetric subsystem. *J.Energy Convers Manage*, *51* (11) ,2272-2278

E. Babaei, S. Alilu, and S. Laali. (2014). A new general topology for cascaded multilevel inverters with reduced number of components based on developed H-bridge. *IEEE Tran Ind Electron*, *61* (8), 3932-3939.

E. Babaei, S. Laali, and S. Alilu. (2014). Cascaded multilevel inverter with series connection of novel H-bridge basic units. *IEEE Trans. Ind. Electron*, *61*(12), 6664-6671.

E. Babaei, S. Laali, and S. Bahravar. (2015). A New Cascaded Multi-level Inverter Topology with Reduced Number of Components and Charge Balance Control Methods Capabilities. *Electric Power Components and Systems*, *43*(1), 2116-2130.

F. S. Hamdad, A. K. and S. Bhat. (2004). Three-phase single-stage AC/DC boost integrated series resonant converter, *IEEE Trans. Aerosp. Electron. Syst*., *40*(4), 1311-1323.

F. Wu , B. Li, and H. B. Gooi. (2017). Principle and control of modified cascaded NPC-GCI with variable topology ability to enhance European efficiency, *IEEE Trans. Ind. Electron*., *64*(2), 1214–1221.

F. Z. Peng, .Z-source inverter. 37th Industry Applications Conference (IAS). *Annual Meeting, Pittsburgh, PA, U. S. A, 69*(2), 775-781, 13-18.

G. Sinha, T. A. Lipo, (2002).A New Modulation Strategy for Improved DC Bus Utilization in Hard and Soft Switched Multilevel Inverters. *In IECON*, . 670-675

G. Yang, P. Dubus, and D. Sadarnac, (2012).Analysis of the load sharing characteristics of the series-parallel connected interleaved LLC resonant converter. *Proc. IEEE Optim. Electr. Electron. Equip.*, 798-805.

H. Krishnaswami, N. Mohan, (2009). Three-Port Series-Resonant DC-DC Converter to Interface Renewable Energy Sources With Bidirectional Load and Energy Storage Ports. *IEEE Transactions on Power Electronics, 24*(10), 2289-2297.

H. Xiao, S. Xie, Y. Chen, and R. Huang. (2011). An optimized Transformerless photovoltaic grid-connected inverter. *IEEE Trans. Ind. Electron*, *58*(5), 1887–1895.

I. Millan, J. M. Burdio, J. Acero, O. Lucia, and S. Llorente,(2011). Series resonant inverter with selective harmonic operation applied to all-metal domestic induction heating. *IET Power Electron.,4*(5), 587-592.

J. H. Kim, I. O. Lee, and G. W. Moon. (2017).Analysis and design of a hybrid-type converter for optimal conversion efficiency in electric vehicle chargers. *IEEE Trans. Ind. Electron,64*(4), 884-893.

J. M. Burdío, F. Monterde, J.R. García, L.A. Barragán, and A. Martínez. (2005).A two-output series-resonant inverter for induction-heating cooking appliances. *IEEE Trans. Power Electronics,20*(4)815-822.

J. Holtz. S. Stadtfeld and P. Lammert, (1985). An economic very high power PWM inverter for induction motor drives. In *European Power Electronics Conf. Rec.,Bruxelles (Belgium*), (vol 50,2, pp 16-18).

J. S. Lai, F. Z. Peng.(1996). Multilevel Converter - A New Breed of Power Converters. *IEEE Transactions on Industrial Applications, 32(3*),517.

K. In-Dong, N. Eui-Cheol, K. Heung-Geun, and K. Jong Sun, (2004). A generalized undelandsnubber for flying capacitor multilevel inverter and converter. *IEEE Trans. Ind. Electron*, *51*(6), 1290-1296.

L. He, C. Cheng, (2016). A Flying-Capacitor-Clamped Five-Level Inverter Based on Bridge Modular Switched-Capacitor Topology. *IEEE Transactions on Industrial Electronics, 63* (12), 7814-7822.

L. Jin, (2009). A novel three-level zero-current-transition active neutral-point-clamped inverter. *In Energy Conversion Congress and Exposition2009. ECCE* 847-852.

Li Zhang, Kai Sun, Lanlan Feng, Hongfei Wu, and Yan Xing. (2013). A Family of Neutral Point Clamped Full-Bridge Topologies for Transformerless Photovoltaic Grid-Tied Inverters. *IEEE Trans. On Power Electron. 28*(2), 730–739.

M. A. Halim, M. N. Hidayat, and M. N. Seroji. (2013). Implementation and analysis of a half-bridge series-parallel LLC loaded resonant DC-DC converter for low power applications. *In Proc. IEEE Power Electron. Drive Syst.*, 634-638.

M. Alam, W. Eberle, D. S. Gautam, C. Botting and N. Dohmeier, and F. Musavi. (2017). A hybrid resonant Pulse-width modulation bridgeless AC–DC power factor correction converter. *IEEE Trans. Ind. Appl., 53*(2), 1406-1415.

M. F. Kangarlu, E. Babaei, and M. Sabahi. (2013). Cascaded cross-switched multilevel inverter in symmetric and asymmetric conditions", *IET Power Electron., 6*(2), 1041-1050.

M. Jabbari. (2010). Resonant inverting-buck converter. *IET Power Electron., 3*(4), 571-577.

M. Kim, H. Jeong, B. Han, and S. Choi. (2018). New Parallel Loaded Resonant Converter With Wide Output Voltage Range. *IEEE Trans. Power Electron., 33*(4), 3106-3114.

M. M. Ghahderijani, M. Castilla, A. Momeneh, J. T. Miret, and L. G. D. Vicuna. (2017). Frequency-modulation control of a DC/DC current-source parallel-resonant converter. *IEEE Trans. Ind. Electron*, *64*(7), 5392–5402.

M.K. Kazimierczuk, D. Czarkowski, N. Thirunarayan. (1993). A New Phase-Controlled Parallel Resonant Converter. *IEEE Trans. Ind. Electronics, 40,* 542-552.

Mohan N., Undeland T.M., and Robbins W.P. (1995). Power Electronics Converters Applications and Design.,(1995), John Wiley & Sons. Inc.(Second Edition), 249-295.

N. A. Rahim, M. F. M. Elias, and W. P. Hew. (2013). Transistor-Clamped H-Bridge Based Cascaded Multilevel Inverter With New Method of Capacitor Voltage Balancing. *IEEE Trans. Ind. Electron*, *60*(8), 2943-2956.

N. Shafiei, M. Ordonez, and W. Eberle. (2014). Output rectifier analysis in parallel and series-parallel resonant converters with pure capacitive output filter. *In IEEE Appl. Power Electron. Conf. Exp* (pp. 9-13) .

Neilor C. Dal Pont , and Telles B. Lazzarin. (2019) .A ZVS APWM Half-Bridge Parallel Resonant DC–DC Converter With Capacitive Output. *EEE Transactions on Industrial Electronics, 66* (7), 5231-5241.

P. Roshankumar, P.P. Rajeevan, and K. Mathew . (2012). A five-level inverter topology with single-DC supply by cascading a flying capacitor inverter and an H-bridge. *IEEE Trans. Power Electron*., *27*(8). 3505-3512.

Prakash Singh Sachin Tiwari, KK Gupta. (2012). A New Topology of Transistor Clamped 5-Level H-Bridge Multilevel Inverter with voltage Boosting Capacity. *In* 2012 *IEEE International Conference on Power Electronics, Drives and Energy Systems* December16-19, 2012, Bengaluru, India.

Q. A. Le, D.-C. Lee. (2016). A novel six-level inverter topology for medium-voltage application. *IEEE Trans. Ind. Electron*., *63*(11).

R. Gonzalez, J. Lopez, P. Sanchis, and L. Marroyo. (2007). Transformerless inverter for single-phase photovoltaic systems. *IEEE Trans. Power Electron*., *22*(2), 693–697.

R. R. Karasani, V. B. Borghate, P. M. Meshram, H. M. Suryawanshi and S. Sabyasachi. (2017).A three-phase hybrid cascaded modular multilevel inverter for renewable energy environment. *IEEE Trans. Power Electron*., *32*(2), 1070-1087.

R. Yang, H. Ding, Y. Xu, L. Yao, and Y. Xiang. (2014).An analytical steady state model of LCC type series-parallel resonant converter with capacitive output filter. IEEE Trans. Power Electron., *29*(1), 328-338.

S. M. Showybul, Islam Shakib and SaadMekhilef. (2017).A Frequency Adaptive Phase Shift Modulation Control Based LLC Series Resonant Converter for Wide Input Voltage Applications. *IEEE Trans. Power Electron.,32*(11), 8360- 8370.

S. M. Tenconi, M. Carpita, C. Bacigalupo, and R. Cali. (1995). Multilevel voltage source converter for medium voltage adjustable speed drives. Proc. ISIE, *IEEE, Athens,* 91.

U. Kundu , S. Chakraborty, and P. Sensarma. (2015). Automatic resonant frequency tracking in parallel LLC boost DC-DC converter. *IEEE Trans.* Power Electron., *30*(7) 3925–3933.

W. Li, Q. Luo, Y. Mei, S. Zong, X. He, and C. Xia. (2016).Flying-Capacitor-Based Hybrid LLC Converters With Input Voltage Autobalance Ability for High Voltage Applications. *IEEE Trans. on Power Electronics,31*(3) 1908-1920.

W. Wu, Y. Sun, Z. Lin, T. Tang and H.S.-H. Chung. (2014).A new LCL-filter with in-series parallel resonant circuit for single-phase grid-tied inverter. *IEEE Trans. Ind. Electron., 61*(9), 4640-4644.

W. Yu, J.S. Lai, and W.-H. La.(2012). Hybrid resonant and PWM converter with high efficiency and full soft-switching range. *IEEE Trans. Power Electron*, *27*(12), 4925-4933.

PLAGIARISM